A GEOMORPHIC CHARACTERIZATION OF AN ECUADORIAN PÁRAMO RIVER

A Thesis
by
CHRISTOPHER PALUMBO ELY

Submitted to the Graduate School
Appalachian State University
in partial fulfillment of the requirements for the degree of
MASTER OF ARTS

August 2017
Department of Geography and Planning

A GEOMORPHIC CHARACTERIZATION OF AN ECUADORIAN PÁRAMO RIVER

A Thesis
by
CHRISTOPHER PALUMBO ELY
August 2017

APPROVED BY:

Derek J. Martin
Chairperson, Thesis Committee

Chuanhui Gu
Member, Thesis Committee

Mike Mayfield
Member, Thesis Committee

Kathleen Schroeder
Chairperson, Department of Geography and Planning

Max Poole
Dean, Cratis Williams Graduate School

Abstract

A GEOMORPHIC CHARACTERIZATION OF AN ECUADORIAN PÁRAMO RIVER

B.A., Southern Illinois University Carbondale
M.A., Appalachian State University
Chairperson: Derek J. Martin

The páramo describes a neo-tropical alpine grassland located between the permanent tree and snowline in the northern Andes of South America. Millions of people in the northern Andes are dependent upon the páramo for ecosystem services. The páramo serves as the principal supply of freshwater for agriculture and consumption as well as hydropower generation and is an important headwater region of the Amazon River. However, very little is known about the hydro-geomorphic characteristics of these river systems that are increasingly being impacted by human use, and climate change. The objectives of this research are to characterize the geomorphology of the Ningar River, a headwater stream in the Amazon basin that drains a 14.52 km^2 páramo watershed in the Central Cordillera of south central Ecuador. This characterization includes establishing hydraulic geometry and stream power relationships derived from topographic surveys and pebble count data, and a subsequent global comparison with other, previously studied mountain river systems. These results will be discussed within the context of implications for hydropower development in páramo ecosystems. Results suggest that páramo streams exhibit similar hydro-geomorphic characteristics as other mountain systems of similar size, as well as grassland and plains areas, likely because ample sediment supply in lower slope reaches in the form of páramo soils. Constructing dams in this environment could disrupt the potentially important geochemical connection between the páramo and downriver ecosystems, such as the Amazon.

Dedication

This thesis is dedicated to my parents. I can't imagine where I would be without their love and support.

Acknowledgments

Special thanks must be given to the Oak Ridge Associated Universities consortium and to the Office of Student Research at Appalachian State University. This project and my involvement with it would not have been possible without financial support from these institutions. Special thanks must also be given to Stu White and the Fundación Cordillera Tropical for their support, insight, and knowledge of the study area and their logistical support. A very special thanks must be given to our driver, Juan Diego Peña for his expertise, punctuality, and entertainment.

Foremost thanks is owed to Dr. Derek Martin for the fantastic research opportunity, his expert advice, and especially the investment of his time. Also for taking me to South America. I would like to thank Dr. Chuanhui Gu and Dr. Mike Mayfield for agreeing to serve on my committee and for providing invaluable insight and criticisms in the pursuit of rigorous science. I also must extend a special thanks to John Wiswell for his research advice and dogged help locating necessary data, and Kaitlin Finan for her GIS help and expertise. I'd also like to thank Robin Hale, the GIS lab supervisor for her timely technical help, and sage advice. And finally, very special thanks must be given to Kathy Brown, Administrative Support Specialist for the Geography and Planning Department. She helped me out of more than a few jams.

Table of Contents

List of Tables

List of Figures

Chapter 1: Introduction

Mountainous regions are important freshwater reservoirs that have been likened to the world's water towers for the disproportionate amount of water they provide (Messerli, Viviroli, & Weingartner, 2004; Viviroli & Weingartner, 2004). This is especially true for South America, the continent that delivers more freshwater to the ocean per square km of land than any other continent (FAO, 2003). Much of this water originates in the Andes Mountains in a unique ecosystem known as the páramo. The páramo is a neotropical grassland ecosystem located above the permanent forest line but below the permanent snow line of the northern Andes of South America (Baruch, 1984; Luteyn, 1999). The páramo is uniquely situated to serve as the water and electric power source for much of the northern Andean region of South America. Additionally, headwater streams in the Andes supply the majority of sediment and nutrient loads to the Amazon River, though they only comprise a fraction of the area of the Amazon basin (Devol & Hedges, 2001; Gibbs, 1967; Luteyn, 1999; Townsend-Small et al., 2008). These vital Andes-Amazon linkages are being threatened by an unprecedented number of dam construction projects occurring in the northern Andes (Buytaert, Célleri, et al., 2006; Célleri & Feyen, 2009; Harden, 2006). Therefore, understanding the hydro-geomorphic intricacies of Andean páramo streams prior to hydro-development is important.

Further, this region is unique among mountain regions as it has been populated for centuries and still contains large population centers that are almost entirely dependent on water originating in the páramo (Buytaert, Célleri, et al., 2006; Harden, 2006). It is surprising then that little research has been dedicated to understanding the hydro-geomorphic processes that drive such an important ecosystem. This research aims to assess the hydro-geomorphic relationships that will help place this potentially unique river system into context with other mountain-region river systems around the

world, thus providing a basis for understanding the implications of human-induced alterations of systems like this throughout the northern Andes.

Páramo Ecosystems

Páramo grasslands follow the Cordilleras of the northern Andes as a discontinuous belt from northern Peru through Ecuador and Colombia into Venezuela, with pockets in Central America (Figure 1).

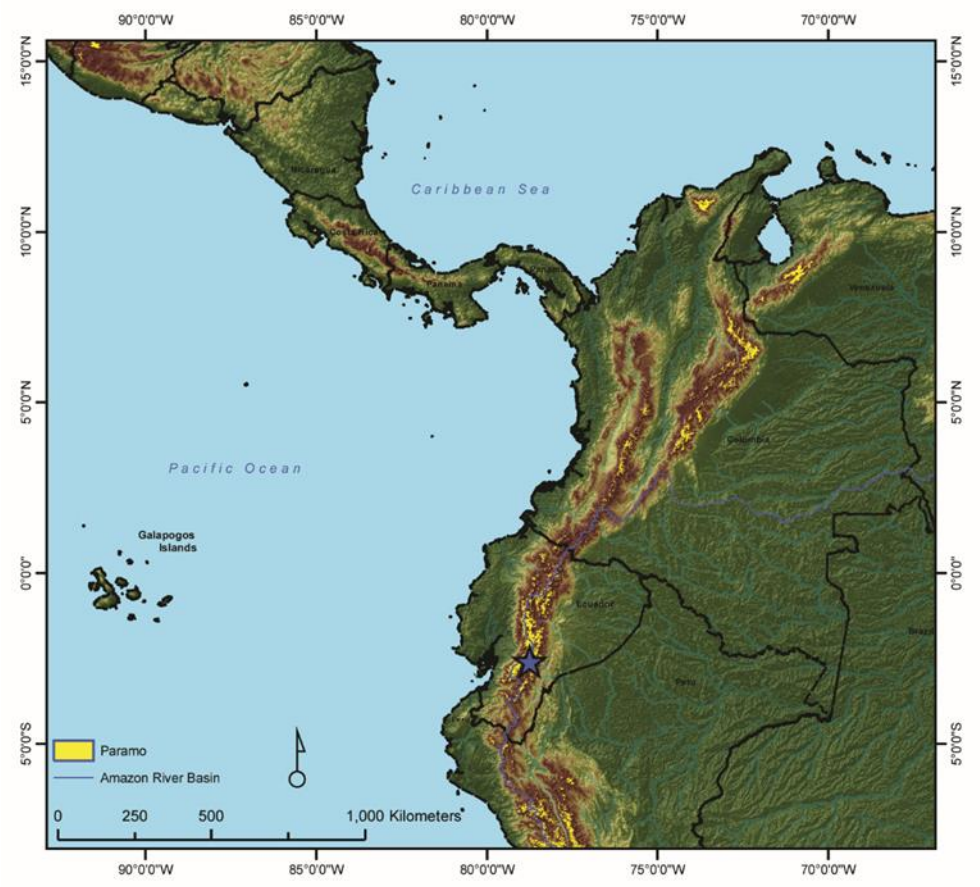

Figure 1. Distribution of the páramo in the neotropics and Central America, and the location of the Ningar River represented as a star.

Comprising 77,000 km^2, the páramo is the dominant ecosystem in the northern Andean region (Dinnerstein et al., 1995), though disagreement exists over the actual extent resulting from confusion in determining the natural tree line (Buytaert, Célleri, et al., 2006; White, 2013). The climate of the

páramo varies by location, but is generally cool and wet because of the elevations they occupy and their locations relative to the Intertropical Convergence Zone. Many páramo areas receive over 2,000 mm of annual rainfall, great diurnal variation in temperatures, and receive high solar energy and ultraviolet input (Luteyn, 1999). The biodiversity of the páramo is low compared to other tropical ecosystems (R. Hofstede, Segarra, & Vásconez, 2003), though the páramo is a relatively young ecosystem and is undergoing a rapid and recent diversification (Madriñán, Cortés, & Richardson, 2013).

The páramo owes its water retention and regulation abilities to its soils (Buytaert, Célleri, et al., 2006; Buytaert, Deckers, & Wyseure, 2006; Poulenard, Podwojewski, & Herbillon, 2003). These soils, which are predominantly andosols (Buytaert, Deckers, & Wyseure, 2007), possess an open and porous structure that affords a high degree of water retention (Buytaert, Deckers, et al., 2006; Crespo et al., 2009; Mena Vásconez & Hofstede, 2006; Poulenard, Podwojewski, Janeau, & Collinet, 2001). This structure is influenced by the high organic content of the soils that result in a low bulk density (Buytaert, Iñiguez, & Bièvre, 2007; Neirop, Tonneijck, Jansen, & Verstraten, 2007). Vegetation in the páramo consists of a vast range of tussock grasses and small woody shrubs depending on the region (Luteyn, 1999) (Figure 2).

Figure 2. Tussock grasses and other vegetation common in the Ecuadorian páramo.

Páramo soils are also an important global carbon sink as reflected by the aforementioned high organic carbon content(Farley, Kelly, & Hofstede, 2004; R. G. M. Hofstede, Groenendijk, Coppus, Fehse, & Sevink, 2002). This sink is a function of lithology and climate. Microbial decomposition of organic material is tempered by the cool and wet climate, and high altitude and solar radiation. The annual mean temperature ranges from 10-12° C and the average precipitation is 1000-2000 mm yr^{-1} (Gade, 1999; Harden, 2006). Frequently saturated soils also inhibit the redox potential (Buytaert, Deckers, et al., 2006). The above mentioned conditions are also favorable to the formation of organometallic complexes incorporating Al and Fe cations as opposed to the formation of clay minerals (Nanzyo, Dahlgren, & Shoji, 1993). The presence of these cations further inhibit decomposition of organic material as they are often toxic to micro-organisms (Buytaert, Deckers, et al., 2006).

Fluvial Geomorphic Assessments

River systems are routinely characterized by their unique relationships between channel geometry, discharge, and drainage area (Rosgen, 1994; Stewardson, 2005). The importance of these at-a-station relationships was originally identified by Leopold and Maddock (1953). They defined these relationships as a stream's hydraulic geometry, and since that time much effort has been expended in attempts to provide greater resolution to those relationships (Bieger, Rathjens, Allen, & Arnold, 2015; Rosgen, 1994). Understanding the hydraulic geometry of a stream is important because, among other things, it informs the shape of flood waves, as well as the stream's material transport capacity, including sediments, nutrients and potential pollutants (Chang, 1988; Richards, 1982; Stewardson, 2005; Western, Finlayson, McMahon, & O'Neill, 1997). In essence, hydraulic geometry refers to the relationships between different discharges and cross-sectional parameters such as width (W_{bf}), depth (D_{bf}), and mean velocity (V_{bf}) (Leopold & Maddock, 1953; Leopold, Wolman, & Miller, 1964). These three variables are known to be related to discharge (Q_{bf}) as simple power functions (Leopold & Maddock, 1953, Equations 1, 2, 3). Since the product of W_{bf}, D_{bf}, and V_{bf} is equal to Q_{bf}, the products of the coefficients of these equations should equal one. The same is true for the sum of the exponents. They are also known to increase with a stream's drainage area (Leopold et al., 1964).

$$W_{bf} = aQ_{bf}{}^{b} \quad \text{Eq. (1)}$$

$$D_{bf} = cQ_{bf}{}^{f} \quad \text{Eq. (2)}$$

$$V_{bf} = kQ_{bf}{}^{m} \quad \text{Eq. (3)}$$

Where:
W_{bf} =bankfull width (m),
D_{bf}=mean bankfull depth (m)
V_{bf}=mean velocity (m/s)
Q_{bf}= bankfull discharge (m^3/s)
while *a,c,k,b,f,m* are all numerical constants

Fluvial geomorphic surveys most often include measurements of bankfull hydraulic geometry. Bankfull discharge refers to the flow that defines the transition between the limits of a

stream's channel and its floodplain (Leopold et al., 1964), and often corresponds to a recurrence interval of 1.5 years (Leopold et al., 1964). Bankfull discharge is understood as the most effective flow for sediment transport, the creation and migration of bars, bends and meanders, and the geomorphological work associated with stream channel dimensions (Dunne & Leopold, 1978). Surveying reaches with respect to bankfull hydraulic geometry will therefore relay information on what is believed to be the most significant discharge.

Geomorphic characterizations serve as the foundation upon which other fluvial research must build, from biology to engineering (Bieger et al., 2015; Dingman, 2007; Rosgen, 1994; Stewardson, 2005). These assessments are necessary for any project that will impact downstream biotic environments and physical processes. Assessments allow managers to incorporate mimicking "natural" conditions in their designs (Gilvear, 1999; Rosgen, 1994). It must be noted though, that there is some disagreement over the extent "natural" conditions can be mimicked, and the degree to which "natural" channel forms predict a stream's response to impairments (Lave, 2009; Miller & Ritter, 1996). The Rosgen Classification is widely employed by federal agencies and the stream restoration community. It is admittedly contentious, yet even ardent critics accept and admit its utility as a communication tool for sharing information among researchers, governments, and private firms (Lave, 2009; Miller & Ritter, 1996).

Mountain Geomorphology

Understanding the hydraulic geometry of mountain streams is often underappreciated, and poorly studied across a range of environments compared to lowland rivers (Montgomery & Buffington, 1997; Viviroli & Weingartner, 2004; E. Wohl & Merritt, 2008). This is surprising given the importance of mountain streams. It is estimated that 40% of the global population is located in watersheds whose headwaters originate in mountainous areas (Beniston, 2003). Catchments in high relief areas contribute a disproportionate amount of sediment that is transported to the oceans (Milliman & Syvitski, 1992). Additionally, these same catchments are often responsible for a

disproportionate amount of streamflow throughout a river network, relative to their length and area (Messerli, Viviroli, Weingartner, 2004; E. E. Wohl, 2000). The geomorphology of tropical mountain rivers is especially important because high rainfall, dense vegetation, and high weathering rates intersect in these regions (Townsend-Small et al., 2008). Globally, rivers with headwaters located in tropical mountain ranges contribute more sediment and nutrients to the oceans than any other type of river system (Milliman & Meade, 1983). The Amazon alone discharges roughly one third of the total discharge to the Atlantic Ocean, at a volume nearly five times greater than the next largest river (Dai & Trenberth, 2002).

Importance and Objective

Water supply is the principle environmental service that the páramo provides for the Andean highlands of Venezuela, Colombia, Ecuador, and large lowland areas (Buytaert, Célleri, et al., 2006; Luteyn, 1999). Over ten million people rely on the páramo as a freshwater reservoir and a comparable number for hydroelectricity (Buytaert, Deckers, et al., 2006; Harden, Hartsig, Farley, Lee, & Bremer, 2013). Further, streams draining páramo ecosystems contribute a substantial amount of sediment, nutrients, and stream flow to the Amazon river to the east, supporting one of the most biodiverse floodplain ecosystems on earth, and to the Pacific coastal plain to the west (Célleri & Feyen, 2009; Luteyn, 1999; Townsend-Small et al., 2008). Many of these streams originate in small páramo catchments similar to the Ningar River watershed where our research sites were located. However, over the past several decades, changing land reform policies have precipitated increased human impacts in the páramo in the form of increased cultivation and grazing activities (Harden, 2006; Harden et al., 2013; Luteyn, 1999), and numerous dams have already been approved for construction to meet the growing water supply and power generation demands in these unique ecosystems, but also of neighboring lowlands as well (Buytaert, Célleri, et al., 2006; Célleri & Feyen, 2009; Finer & Jenkins, 2012).

The overall objective of this research is to characterize and quantify channel form in the Ningar River, Ecuador, which drains a páramo grassland ecosystem. Specific objectives include:

(1) Quantify channel geometry

(2) Describe longitudinal channel characteristics

(3) Establish hydraulic geometry and stream-power relationships

(4) Perform a global comparison with mountain river systems

This research is important because it will serve as a first step toward understanding the hydro-geomorphic function and characteristics of páramo streams by contributing to the extremely limited body of knowledge regarding Andean páramo fluvial systems. Additionally, this research will supply critically important pre-dam hydro-geomorphic data that can be used to perform post-dam analyses of environmental impacts and potentially help establish post-dam management of flow conditions. Further, collecting baseline hydro-geomorphic data in this region is important given the area's susceptibility to climate change and anthropogenic impacts in light of the large and growing populations that depend on the páramo as a water and electricity source, and the influence these headwater catchments have in larger drainage networks (Bradley, Vuille, Diaz, & Vergara, 2006; Buytaert, Célleri, et al., 2006; Harden, 2006; R. G. M. Hofstede et al., 2002; E. Wohl & Merritt, 2008).

The results from these analyses and the known location of the approved dam on the Ningar River will inform discussions of the potential implications of dam construction in this environment. Placing the Ningar River into context with other well-known mountain river systems will allow for a better understanding of the sediment/nutrient transport capacities, flow regimes, and the overall geomorphic capacities of this system. Further, these results will also play an important role in ongoing research that aims to understand fluvial organic carbon flux from páramo ecosystems.

Chapter 2: Study Area

The Ningar River (Figures 3, 4) is a 7.3km long headwater stream of the Amazon River basin located in the Central Cordillera in the Cañar province of south central Ecuador (Harden et al., 2013; Potable, 2012). The Ningar watershed is 14.52 km^2 (Figure 5) and drains a large portion of the Mazar Wildlife Preserve which is managed by the Fundación Cordillera Tropical (FCT), who provided the following land use data. Nearly 62% of the watershed is classified as páramo, primarily covered by tussock grasses and shrubs, while montane and shrub forests, and several stands of cultivated *pinus patula* trees comprise another 30%. The watershed is nearly devoid of any cultivated agricultural land and 2.95% of the watershed is defined as working fields in good condition. However, 2.53% of the watershed has been burned recently to facilitate the grazing of cattle. The watershed is underlain by marine sedimentary rocks of the Mesozoic Yunguilla formation (Bristow, 1973; Hungerbuhler et al., 2002). Soils in the Ningar watershed are comprised of histic hydrandepts and cryandepts (Yanchapaxi, Miranda, Colmet-Daage, & Zebrowski, 1983), contributing to the incredible water holding capacity, and carbon storage capacity of the páramo (Buytert, Deckers, et al., 2006; Harden et al., 2013).

Figure 3. Ningar River looking upstream from near the location of the future dam.

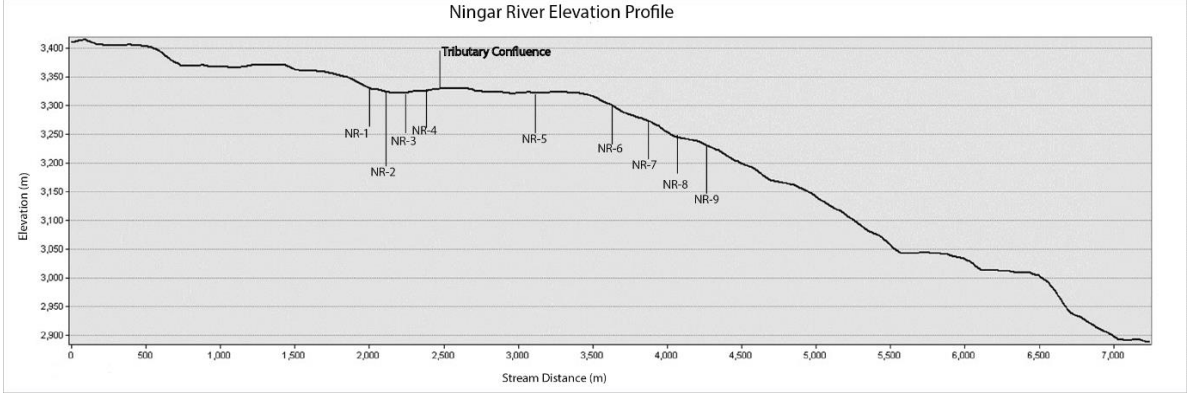

Figure 4. Ningar River elevation profile showing the location of the survey sites and tributary location.

Of interest is the planned construction of a multifunctional dam in the watershed as part of an effort to meet the freshwater consumption, irrigation, and electricity needs of the cities of Azogues and Paute, as well as dozens of towns and communities in both the Burgay and Paute basins for the next 20 years. The dam will be located at the confluence of the Ningar River and the Ullapungo ravine, roughly the location of survey site NR-6. With an expected height of 25 m, the dam is estimated to create a reservoir with a storage capacity of 2.5 million m^3 with a mean regulated flow of .373 m^3/s (EMAPAL, 2012).

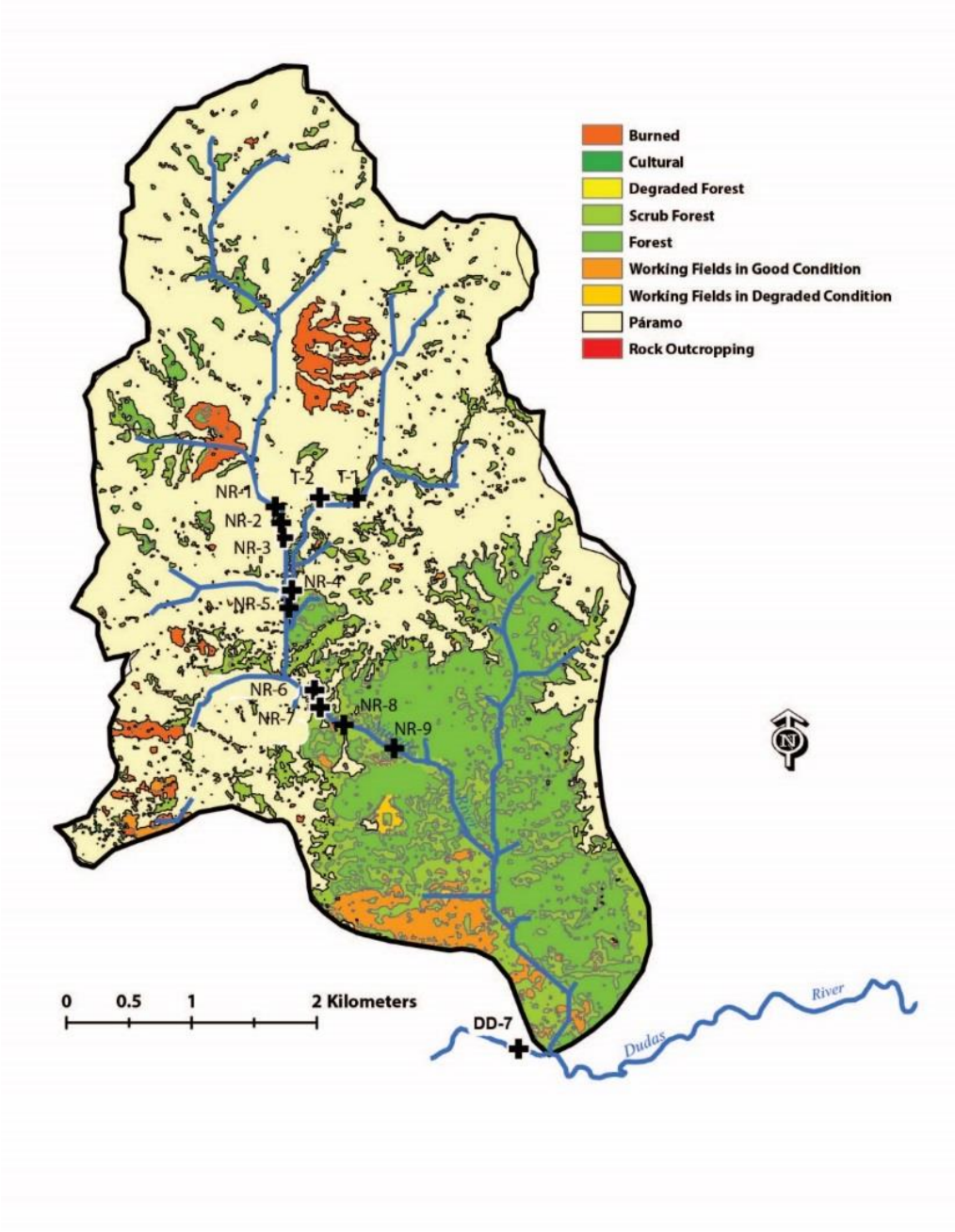

Figure 5. Ningar watershed showing survey locations and land cover (provided by FCT).

Chapter 3: Methods

Field Methods

To characterize the geomorphology of the upper Ningar River, geomorphic assessments were conducted at 11 sites along the river and were acquired over three visits. Nine sites were located on the mainstem of the Ningar, while two sites were located on one of the largest tributaries. With the exception of one site, all reaches were located in páramo. Assessments consisted of channel geometry measurements with respect to bankfull conditions, and substrate measurements. These methods were adapted from established sources (Leopold et al., 1964; Rosgen, 1994; Wolman, 1954). Channel geometry measurements included three cross sectional surveys at riffles and a longitudinal survey spanning all three riffles using common rod-and-level channel surveying techniques. An auto-level was used to survey the cross-sectional and longitudinal profiles for the first six reaches during the summer of 2015. To expedite the logistics of the subsequent trips, a hand level was used to survey the final five reaches in the winter of 2015-2016, and 2016-2017. The feasibility of using the hand level was tested in the fall of 2015 by comparing cross-sections that were surveyed using each instrument at a headwater stream in the southern Appalachian Mountains. Comparisons showed only a 2.3% difference between cross-sectional area measurements and were thus deemed satisfactory (Figure 6). Substrate measurements were achieved using a modified Wolman Pebble Count (Wolman, 1954). Counts were conducted across four channel cross sections upstream and four channel cross sections downstream of each surveyed cross-section, for a total of 24 pebble count cross sections per study site.

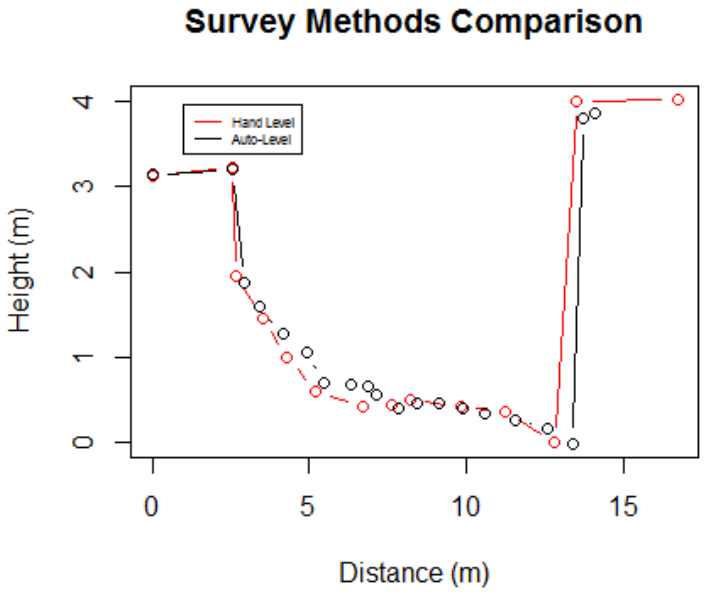

Figure 6. A cross section that was measured using two surveying techniques to demonstrate the feasibility of using a hand level vs. an auto-level to expedite logistics in the field.

Data Analysis

All data analysis was performed in the R software package(R Core Team, 2016). The following variables were extracted from the field data to develop the necessary hydraulic geometry relationships: bankfull width (W_{bf}), mean bankfull depth (D_{bf}), bankfull velocity (V_{bf}), and bankfull discharge (Q_{bf}) (Eq. 4), bankfull boundary shear stress (τ_0) (Eq. 5), critical shear stress (τ_c) (Eq. 6), and stream power (Ω) (Eq. 7). Bankfull velocity was estimated using Manning's equation (Eq. 8). Additionally, a Rosgen Level II classification was performed. This classification examines the width/depth ratio (*W:D*), slope (*S*), entrenchment ratio (*ER*), sinuosity (k), and bed material. Further classification was limited by the resolution of the available GIS data.

$$Q_{bf} = W_{bf} D_{bf} V_{bf} \quad \text{Eq. (4)}$$

$$\tau_0 = \gamma R S \quad \text{Eq. (5)}$$

$$\tau_c = \tau_c^*(\rho_s - \rho_w) g D_{50} \quad \text{Eq. (6)}$$

$$\Omega = \gamma Q S \quad \text{Eq. (7)}$$

$$V_{bf} = \frac{R^{2/3}\sqrt{S}}{n} \quad \text{Eq. (8)}$$

Where:
Q_{bf}= bankfull discharge
τ_0= bankfull boundary shear stress (Pa)
γ= the unit weight of water (N/m^3)
R= the hydraulic radius (m)
S= slope (m/m)
τ_c= critical shear stress (Pa)
ρ_s= density of the sediment (kg/m^3)
ρ_w= density of water (kg/m^3)
τ_c^* is dimensionless critical stress
g= the gravitational constant (9.81 m/s^2)
D_{50} is the median particle size (m)
Ω= stream power (N/s)
n= Manning's Roughness Coefficient
(Leopold & Maddock, 1953; Rosgen, 1994; E. E. Wohl & Wilcox, 2005)

The mentioned above variables were regressed on drainage area and discharge to develop regional curves that could be compared with regional curves already developed for mountainous regions around the world. However, due to limitations in available data, only the W_{bf} and D_{bf} curves were used in our global comparison. Additionally, a Rosgen Level II classification was performed to explore the applicability of this system in the páramo environment. ArcGIS® 10.3 software by Esri, was used to determine the drainage areas for each sub-basin defined by each sample reach.

Chapter 4: Results and Discussion

Bed Morphology

The Ningar River exhibits a variety of stream morphologies along the mainstem and tributary sites. Three different stream morphologies were observed along its relatively short length. Five of the nine main stem reaches classify as riffle pool morphology, two classify as step pool morphology and two classify as cascade morphology. Tributary sites both classify as step pool morphology. For riffle pool reaches the average riffle spacing is 22.93 m while the average residual pool depth is .368 m with standard deviations of 4.69 m and .159 m respectively. In step pool reaches the average step height is .543 m with a standard deviation of .127 m. The average step wavelength is 16.33 m with a standard deviation of 5.17 m. The average slope for the two cascade reaches is .072. A summary of the geomorphic data for each site is found in Table 1.

Table 1. Average Geomorphic Site Characteristics.

Site #	A_d (km^2)	Q_{bf} (m^3/s)	Slope (m/m)	A_{bf} (m^2)	W_{bf} (m)	D_{bf} (m)	W:D	Classification
NR-1	5.60	6.21	.021	3.24	5.61	.55	10.27	Riffle Pool
NR-2	5.61	4.99	.027	2.21	3.54	.57	6.18	Riffle Pool
NR-3	5.92	4.24	.019	2.05	3.60	.57	6.58	Riffle Pool
NR-4	5.99	4.05	.012	2.77	5.01	.57	7.5	Riffle Pool
NR-5	11.89	4.10	.007	3.22	4.27	.70	6.1	Riffle Pool
NR-6	13.67	6.05	.026	3.45	4.73	.73	7.18	Cascade
NR-7	13.69	6.39	.032	2.79	4.28	.62	6.95	Step Pool
NR-8	13.71	8.58	.023	4.43	4.93	.73	6.76	Step Pool
NR-9	14.15	24.32	.117	6.13	7.33	.82	8.86	Cascade
T-1	3.30	4.29	.046	1.55	2.27	.56	4.04	Step Pool
T-2	3.43	2.26	.033	1.15	2.33	.49	4.75	Step Pool

Note. A_d =drainage area, A_{bf} = bankfull cross sectional area, W_{bf} =bankfull width, D_{bf} = bankfull depth, W:D= width depth ratio.

Drainage Area Relationships

Models relating drainage area to bankfull channel geometry and bankfull discharge were created using site-averaged values for each variable. These relationships are typically modeled as power

functions of the form $y=a(x)^b$. The following power relationships for drainage area have been developed for our sites on the Ningar River:

$W_{bf}=1.942(A_d)^{.388}$

$D_{bf}=0.371(A_d)^{.254}$

$A_{bf}=0.74(A_d)^{.655}$

$Q_{bf}=0.773(A_d)^{.998}$

Where:
A_d = drainage area (km^2)
W_{bf} = bankfull (m)
D_{bf}= average bankfull depth (m)
A_{bf}=bankfull channel area (m^2)
Q_{bf}= bankfull discharge (m^3/s)

Data used to create the above models can be seen in Figure 7. Table 2 shows the model coefficients along with model diagnostic information. As seen in Table 2, D_{bf} is the parameter with the best fit to A_d area (r^2=.785), though the relation between bankfull width and drainage area is also well defined (r^2=0.601). Site NR-1 is located just below the mouth of a deeply incised gorge, and may account for the wider W_{bf} at this site. The anomalous W_{bf} at NR-1 has a commensurate effect on the A_{bf} and Q_{bf} relation to A_d for NR-1. Sites NR-3, 4, and 5 have less steep slopes, likely a result of a lithologic control. The negative change in slope helps to explain the poor fit for the Q_{bf} and A_d model (r^2=0.47). The poor model fit for A_{bf} and A_d (r^2=0.27) can be explained by the inherent variability of step pool and cascade morphologies, both of which constitute the larger A_d sites.

Table 2. Model parameters and diagnostics for drainage area relationships.

Model*	A (p-val.)	B (p-val.)	Residual Error	R^2
$W_{bf}=1.942(A_d)^{.388}$	0.0213	0.0344	1.135	0.601
$D_{bf}=0.371(A_d)^{.254}$	5.78E-06	0.00044	0.051	0.785
$A_{bf}=0.74(A_d)^{.655}$	0.076	0.0125	0.944	0.2731
$Q_{bf}=0.773(A_d)^{.998}$	0.54	0.14	5.317	.4733

Note. W_{bf} =bankfull width (m), D_{bf}= bankfull depth (m), A_{bf}= bankfull cross sectional area (m^2), Q_{bf}= bankfull discharge (m^3/s), and A_d=drainage area (km^2).

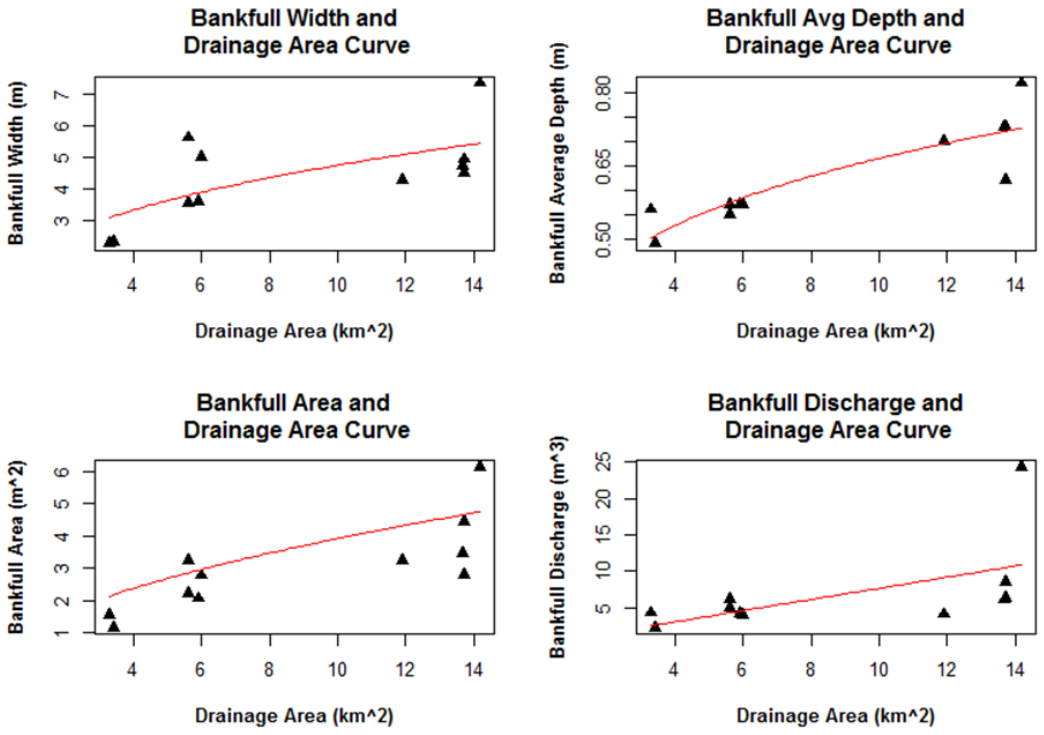

Figure 7. Drainage area relationships with bankfull geometry and discharge.

Discharge Relationships

Models relating bankfull discharge to bankfull channel geometry and velocity were created using site-averaged values for each variable. Like drainage area, these relationships are typically modeled as power functions $y=a(x)^b$ and have been done so here as well. The following power relationships for bankfull discharge have been developed for the sites on the Ningar River:

$W_{bf}=2.19(Q_{bf})^{.387}$

$D_{bf}=0.443(Q_{bf})^{.199}$

$V_{bf}=1.11(Q_{bf})^{.420}$

$A_{bf}=1.12(Q_{bf})^{.548}$

Where:
W_{bf} = bankfull width (m)
D_{bf}= average bankfull depth (m)
V_{bf}= bankfull velocity (m/s)
A_{bf}=bankfull area (m^2)
Q_{bf}= bankfull discharge (m^3/s)

Data used to create the above models can be seen in Figure 8. Table 3 contains the model coefficients along with model diagnostic information. The Q_{bf} models fit the observed data more closely than the other derived relationships. Sites T-1, 2 are incised resulting in deviation from the model for W_{bf}. Sites NR-5, 6, and 7 deviate from the model for D_{bf}. This is likely a result of the transition from the riffle pool to step pool morphologies through the markedly increased slope at NR-6. This increase in slope likely occurs as a change in lithology. The Ningar River is increasingly contained at sites evidenced by the decreasing W:D and entrenchment ratio, and can be seen visually in Figure 9. The decreased A_{bf} and W_{bf} for site NR-7 is likely an artifact of the cascade morphology of NR-6. There is strong agreement between the V_{bf} and Q_{bf} model (r^2=.480). An equal number of sites lie above and below the curve. The variability in the V_{bf} is a partly a function of the decreased slopes at NR-3, 4, and 5 and the increased slopes at the cascade morphology sites.

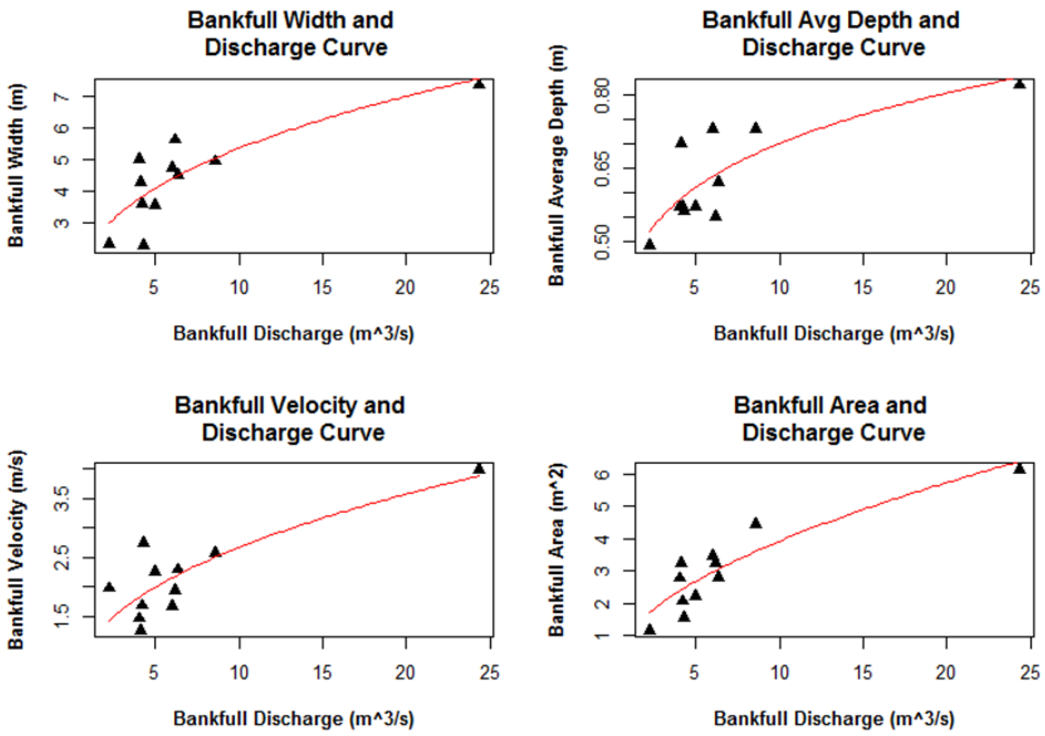

Figure 8. Relationships between bankfull geometry and discharge.

There is strong agreement between the coefficients for our Q_{bf} models and the mathematical derivation proposed by Leopold and Maddock; the exponent coefficients for the W_{bf}, D_{bf}, and V_{bf} models nearly sum to one. Additionally, the product of the algebraic coefficients for these models are nearly equal to one in agreement with Leopold and Maddock. This can be taken as tacit evidence that the methods used for this research are valid for this ecosystem, at least for similar reaches of the surveyed Ningar.

Table 3. Model parameters and diagnostics for discharge relationships

Model*	A (p-val.)	B (p-val.)	Residual Error	R^2
$W_{bf}=2.19(Q_{bf})^{.387}$	0.0003	0.0009	.857	0.601
$D_{bf}=0.443(Q_{bf})^{.199}$	2.02E-06	0.002	0.064	0.627
$V_{bf}=1.11(Q_{bf})^{.420}$	.0005	.0008	.462	.480
$A_{bf}=1.12(Q_{bf})^{.548}$	0.0003	5.75E -05	0.627	0.743

Note. W_{bf} =bankfull width, D_{bf} = bankfull depth (m), V_{bf}= bankfull velocity (m/s), A_{bf} = bankfull cross sectional area (m^2), Q_{bf} = bankfull discharge (m^3/s).

Figure 9. View of future dam location and downstream of NR-6 showing increased incision.

Stream Power and Shear Stresses and Discharge Relationships

Models relating bankfull discharge to bankfull hydraulic parameters were created using site-averaged values for each variable. As above, these relationships are typically modeled as power functions

$y=a(x)^b$ and have been done so here as well. The following power relationships have been developed for discharge with stream power and shear stresses for our sites on the Ningar River:

$\Omega = 27.21(Q_{bf})^{2.16}$

$\tau_0 = 14.865(Q_{bf})^{1.23}$

$\tau_c = 44.3(Q_{bf})^{.099}$

Where Ω = stream power (N/s),
τ_0 = boundary shear (Pa),
τ_c= critical shear (Pa),
Q_{bf}= bankfull discharge (m^3/s).

Data used to create the above models can be seen in Figure 10. Table 4 contains the model coefficients along with model diagnostic information. There is strong agreement for the model relating Ω and Q_{bf} (r^2=0.75), and is one of the strongest fit for any individual model. Conversely, the relationship for τ_c is the weakest fitting individual model (r^2=0.01). NR-8 has the highest τ_c (103.3 Pa), substantially larger than NR-9 (48.7 Pa), the site with the greatest Q_{bf} (24.3 m^3/s)**.** This is a result of large D_{50} measurements for the NR-8 site, likely a condition of this sites location within a narrow entrenched valley. The sample used to calculate the D_{50} for NR-9 was not a complete sample and may account for the less than expected τ_c, though field evidence showed imbricated cobbles and recent physical weathering of in-channel boulders, suggesting frequent entrainment of large materials at NR-9 (Figure 11). The greatest deviation from the curve defined for τ_0 occurs for sites NR-2 above the

curve, and sites NR-3, 4, and 5 below the curve. The largest control on these deviations is slope, which is likely a lithologic control.

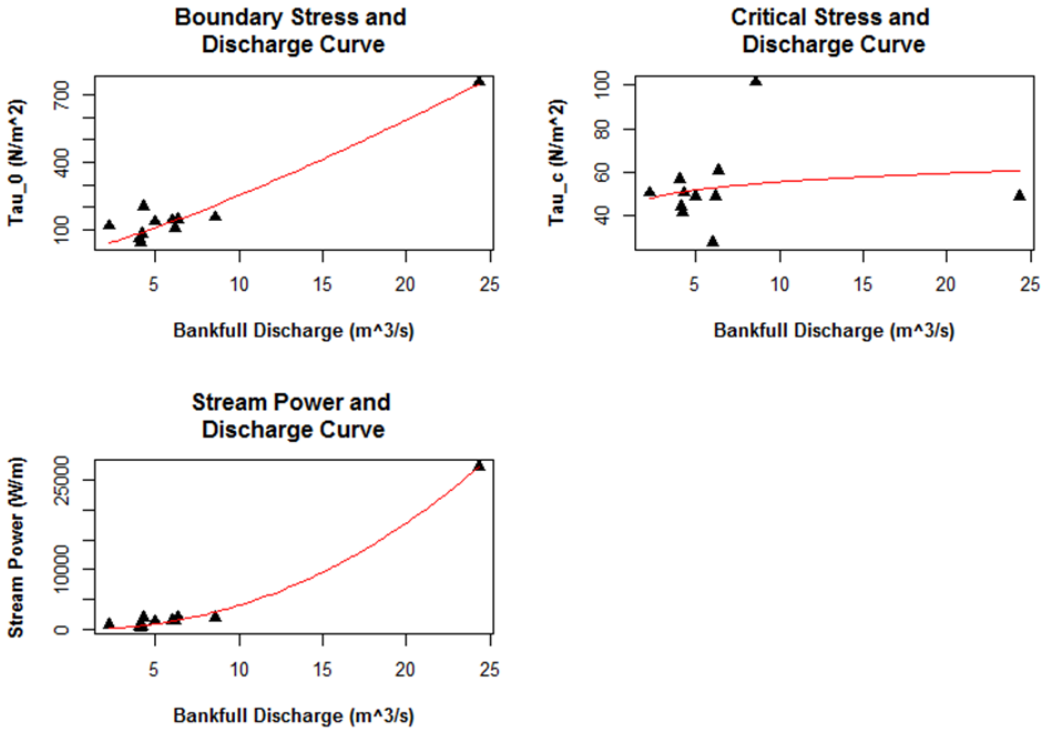

Figure 10. Hydraulic variables and discharge curves.

Figure 11. Evidence of large particle entrainment at NR-9.

Stream power decreases substantially between NR-1 and NR-5 located just upstream of the future dam location. Possible implications for the future dam could be decreased erosion for that stretch of the Ningar River. Conversely, it may also result in increased deposition with potential ramifications for reservoir storage capacity and the operation life-time of the future dam. In this same vein, erosion downstream of the dam could be reduced as NR-8 contains the highest τ_c requiring more energy for incipient particle movement. This is less likely to occur under controlled outflows. Considering this there is the potential for a disruption of the natural sediment supply which will have impacts far beyond the length of the Ningar River.

Table 4. Model parameters and diagnostics for hydraulic variables relationships

Model*	A (p-val.)	B (p-val.)	Residual Error	R^2
$\Omega = 27.2(Q_{bf})^{2.16}$	.0310	2.95E-08	631.7	.745
$\tau_0 = 14.87\ (Q_{bf})^{1.23}$	.0140	1.68E-06	53.82	.575
$\tau_c = 44.3(Q_{bf})^{.099}$	.0155	.589	18.89	.01

Note. Ω =stream power (N/s), τ_0 = bankfull boundary shear stress (Pa), τ_c = critical shear stress (Pa), Q_{bf} = bankfull discharge (m^3/s).

Regional Comparisons

Rosgen Level II Classification

The Mainstem of the Ningar River is most like the B3 or G3 classifications per the Rosgen level II criteria classification. There is agreement between the Ningar River and the B3 classification for slope, entrenchment ratio, sinuosity, and bed material, though the width/depth ratio is markedly less than the expected value per the Rosgen classification criteria for a B3 stream. For the G3 classification, the Ningar River accords well with the slope, width/depth ratio, sinuosity, and bed material, but has a greater than expected entrenchment ratio for this classification. Both stream classifications occur in similar valley types dominated by vegetated colluvial and alluvial fans. The significant difference between the two classifications is that the G stream type occurs in non-equilibrated and unstable environments. The averaged values used to define the classification criteria can be found in Table 5.

Table 5. Site averaged values used for Rosgen Level II Classification

Avg. *W:D*	Avg. Slope	Avg. *ER*	Avg. Sinuosity	Bed Material
7.5	.03	1.56	1.19	Cobble

Regional Curves

Two different data sets were used to create the curves relating W_{bf} and D_{bf} to Q_{bf} and A_d. Although few regions had overlapping datasets, the two datasets provided fourteen and six curves respectively, derived for an equal number of physiographic regions. Important visual inspection can be made by plotting the Ningar River curves along with curves derived from these datasets. Figure 12 contains the

curves relating W_{bf} to Q_{bf} and the equations of the curves for the Q_{bf} relationships and their sources can be seen in Table 6. The Ningar River (NR), represented by the red curve for all plots, retains low W_{bf} values compared to the five other curves. The greatest similarity to the curve for NR is represented by the curve representing northwest Colombia (COL) (Mejía & Posada, 2002). With regards to the D_{bf} and Q_{bf} curves (Figure 13) there is greater similarity among the sample. The magnitude of the NR curve is greater than most, indicating increased incision for páramo streams. Only the Colombia (COL) and Australia (AUS) curves see greater increases in D_{bf} with increased Q_{bf}, though the coefficient for the NR is greater than AUS. The W_{bf} and A_d curve for NR (Figure 14) most closely approximates the curves created using data from the Atlantic Coastal Plain (APL) and Pacific Northwest (PNW) physiographic provinces. The curve for the Interior Plains (IPL) is the next closest approximation. The D_{bf} and A_d curve for the NR (Figure 15) is most closely approximated by the Laurentian Upland Plateau (LUP) and Interior Plains (IPL) physiographic provinces and the New Zealand (NZD) curves, all of which had the greatest D_{bf} relative to A_d of the entire sample. This indicates that the stream banks of these areas are comprised of cohesive materials. The equations of these curves and the source for the data used can be found in Table 7.

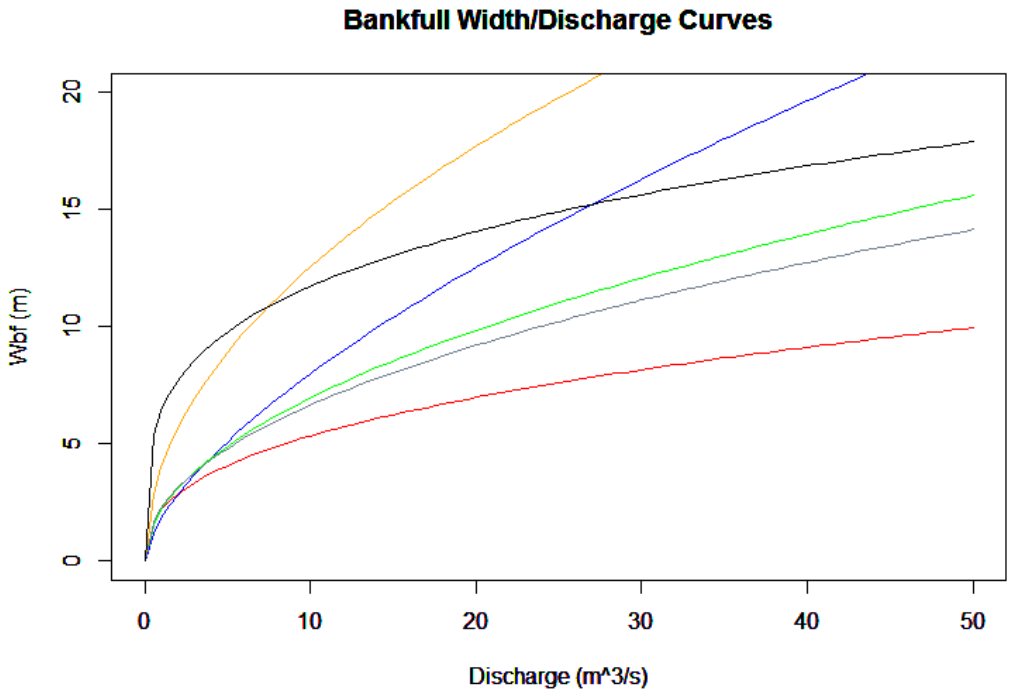

Figure 12. Power relations for bankfull width and bankfull discharge for several different regions. The NR curve was created from data from the Ningar River, NEP was created from data collected in Nepal, NZD from New Zealand, PNW from the Pacific Northwest, COL from Colombia, and AUS from Australia.

Table 6. Data used for Bankfull Discharge regional comparisons

Name	Region/Country	W_{bf}=	D_{bf}=	n	Q_{bf} (m^3/s)	Source
NR	S. Ecuador	$2.19(Q_{bf})^{.387}$	$.443(Q_{bf})^{.199}$	11	2.3-24.3	This Study
NEP	Himalayan Nepal	$1.80(Q_{bf})^{.648}$	$.286(Q_{bf})^{.260}$	42	.6-19.7	(Caine & Mool, 1981)
PNW	Pacific Northwest	$4.02(Q_{bf})^{.495}$	$.259(Q_{bf})^{.385}$	74	3.9-1122	(Castro & Jackson, 2001)
NZD	New Zealand	$2.2(Q_{bf})^{.501}$	$.273(Q_{bf})^{.313}$	34	1.3-193.8	(E. E. Wohl & Wilcox, 2005)
COL	NW. Colombia	$2.26(Q_{bf})^{.469}$	$.57(Q_{bf})^{.335}$	29	8.7-665.8	(Mejía S. & Posada G., 2002)
AUS	SE Australia	$6.42(Q_{bf})^{.262}$	$.134(Q_{bf})^{.65}$	30	3.6-114	(Huang & Nanson, 1997)

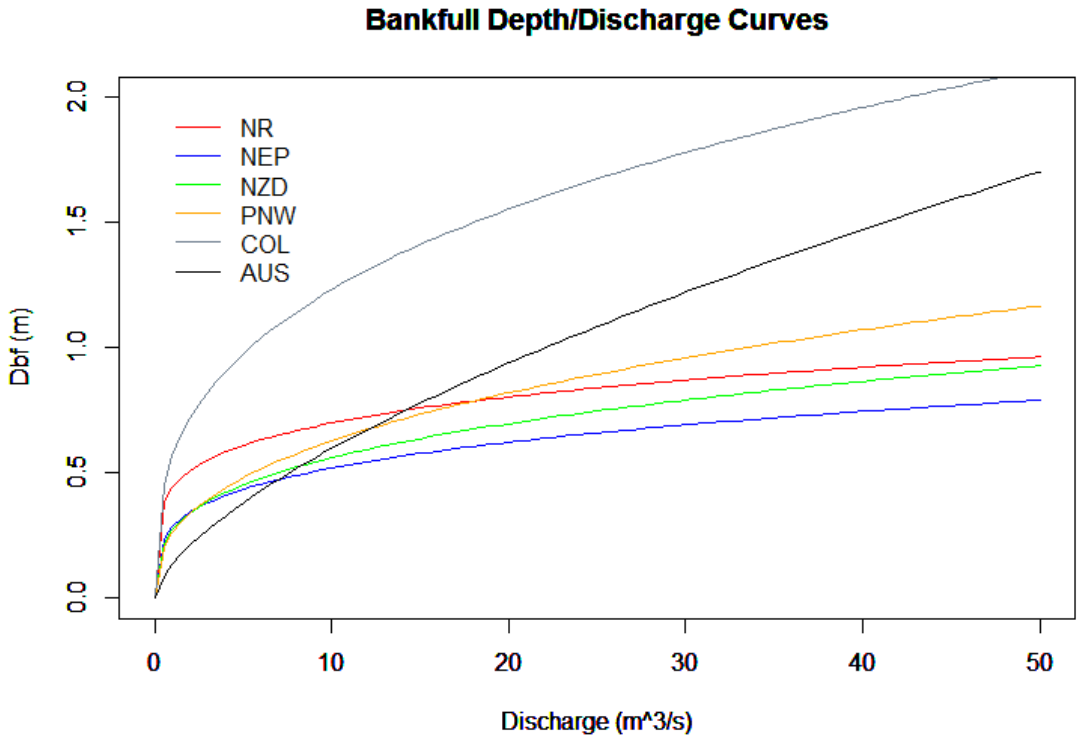

Figure 13. Power relations for bankfull depth and discharge for several different regions. The NR curve was created from data from the Ningar River, NEP was created from data collected in Nepal, NZD from New Zealand, PNW from the Pacific Northwest, COL from Colombia, and AUS from Australia.

The curves that approximated the Ningar River are varied in their physiographic and geographic extent. The similarity between the APL and IPL W_{bf} and A_d curves is unexpected given the vast difference in elevation and topography, but can likely be explained by the abundance of soils and dense grass cover in the Ningar watershed. Among mountain systems, the Ningar can be said to most closely resemble the PNW given the similarities between the W_{bf} and A_d and D_{bf} and Q_{bf} curves. However, the large discrepancy between the W_{bf} and Q_{bf} and D_{bf} and A_d is interesting to note. Where the slope is low, the Ningar River, and páramo rivers in general, can be expected to behave similarly to other grassland areas on account of the abundant vegetation. However, when increased slopes are encountered páramo rivers can be expected to behave more similarly to mountainous areas with large precipitation volumes.

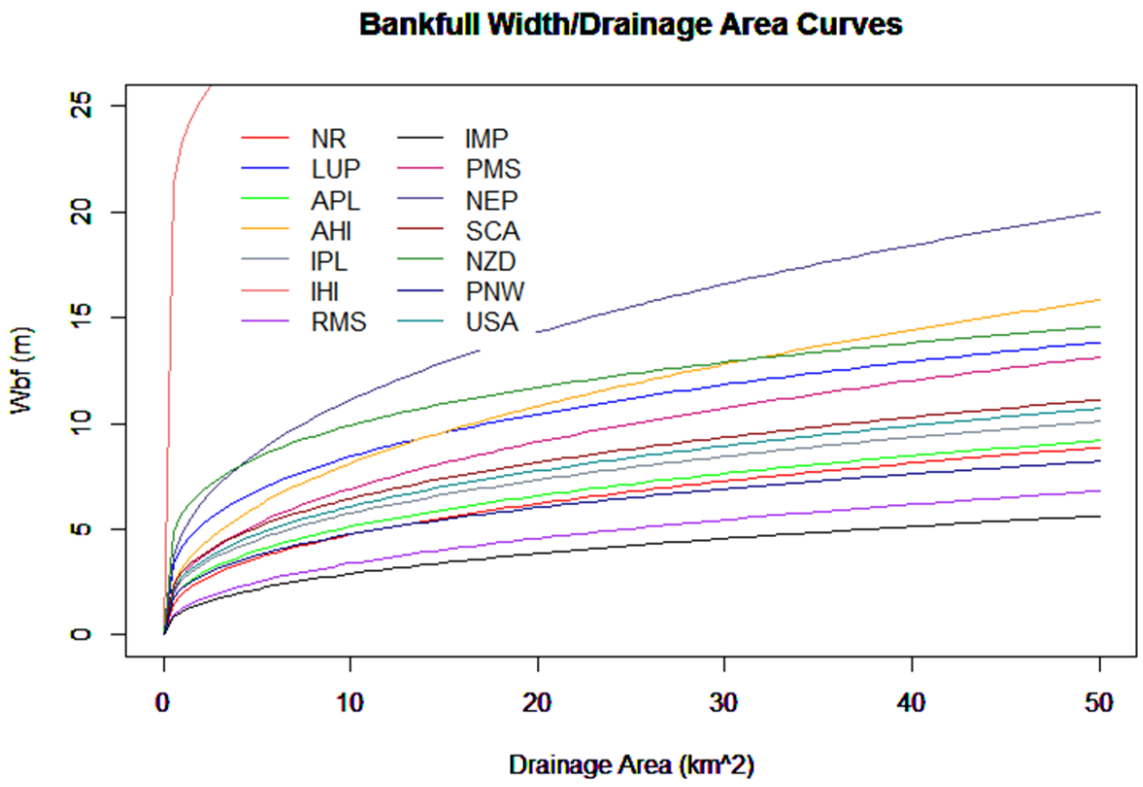

Figure 14. Power relations for bankfull width and drainage area for the physiographic regions of the USA and other areas. NR was created from data for the Ningar River, LUP from the Laurentian Upland Plateau, APL from the Atlantic Coastal Plain, AHI the Appalachian Highlands, IPL the Interior Plains, IHI from the Interior Highlands, RMS the Rocky Mountain System, IMP from the Intermontane Plateau, PMS the Pacific Mountain System, NEP from Nepal, SCA from Southern California, NZD from New Zealand, PNW from the Pacific Northwest, and USA the average for the United States.

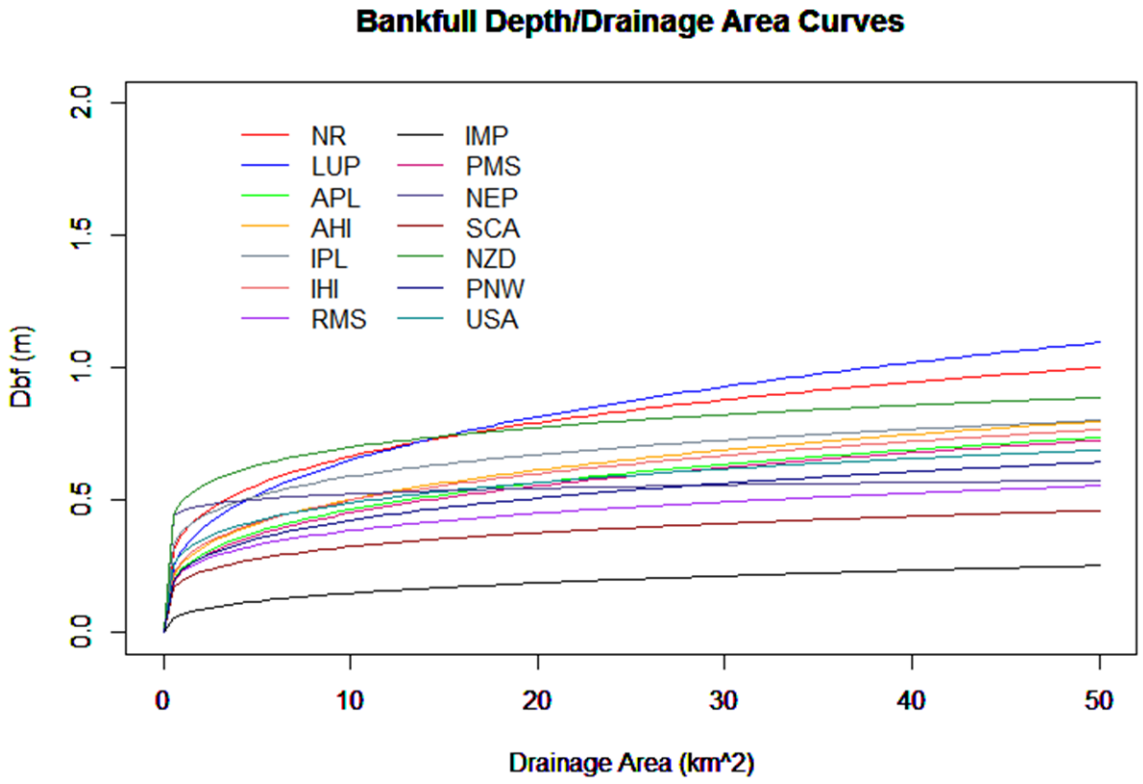

Figure 15. Power relations between depth and drainage area comparing the Ningar River to physiographic regions of the USA and other areas. NR was created from data for the Ningar River, LUP from the Laurentian Upland Plateau, APL from the Atlantic Coastal Plain, AHI the Appalachian Highlands, IPL the Interior Plains, IHI from the Interior Highlands, RMS the Rocky Mountain System, IMP from the Intermontane Plateau, PMS the Pacific Mountain System, NEP from Nepal, SCA from Southern California, NZD from New Zealand, PNW from the Pacific Northwest, and USA the average for the United States.

Table 7. Data used for regional Drainage Area comparisons

Name	Region/Country	W_{bf}=	D_{bf}=	n	A_d (km^2)	Source
NR	S. Ecuador	$1.942(A_d)^{.388}$	$.371(A_d)^{.254}$	11	3.3-14.2	This Study
LUP	Laurentian Upland Plateau	$4.15(A_d)^{.308}$	$.31(A_d)^{.323}$	6	43-948	(Bieger et al., 2015)
APL	Atlantic Coastal Plain	$2.22(A_d)^{.363}$	$.24(A_d)^{.287}$	61	.8-2815	(Bieger et al., 2015)
AHI	Appalachian Highlands	$3.12(A_d)^{.415}$	$.26(A_d)^{.287}$	387	.2-2435	(Bieger et al., 2015)
IPL	Interior Plains	$2.56(A_d)^{.351}$	$.38(A_d)^{.191}$	425	.5-155,213	(Bieger et al., 2015)
IHI	Interior Highlands	$3.23(A_d)^{.121}$	$.27(A_d)^{.267}$	7	78-2484	(Bieger et al., 2015)
RMS	Rocky Mountain System	$1.24(A_d)^{.435}$	$.23(A_d)^{.225}$	288	.4-25,201	(Bieger et al., 2015)
IMP	Intermontane Plateau	$1.11(A_d)^{.415}$	$.07(A_d)^{.329}$	88	9.4-19,632	(Bieger et al., 2015)
PMS	Pacific Mountain System	$2.76(A_d)^{.399}$	$.23(A_d)^{.294}$	48	16-20,927	(Bieger et al., 2015)
NEP	Himalayan Nepal	$4.79(A_d)^{.365}$	$.46(A_d)^{.057}$	42	.02-13.7	(Caine & Mool, 1981)
SCA	Southern California	$2.96(A_d)^{.338}$	$.196(A_d)^{.219}$	31	.5-52.9	(Modrick & Georgakakos, 2014)
PNW	Pacific Northwest	$2.18(A_d)^{.339}$	$.234(A_d)^{.259}$	74	45.8-20,927	(Castro & Jackson, 2001)
NZD	New Zealand	$5.72(A_d)^{.239}$	$.498(A_d)^{.148}$	34	.5-70.3	(E. E. Wohl & Wilcox, 2005)l
USA	United States	$2.7(A_d)^{.352}$	$.3(A_d)^{.213}$	1310	.2-155,213	(Bieger et al., 2015)

Limitations

The results of this research are encouraging, however this analysis is limited by several limitations and potential sources of error. The remote nature of the study area made surveying the upper and lower reaches of the Ningar River logistically problematic. Therefore, the cross-sections are limited to reaches that could be feasibly surveyed and do not capture the entire variability of geomorphic

conditions on the Ningar River. Additionally, site NR-9 is not a complete survey. However, all but one of the sites are located within the páramo and therefore results are still considered representative of páramo geomorphology. Further, the bankfull parameters must be estimated based upon subjective field interpretations and determinations and not on definite criteria (Rosgen, 1996). These estimated bankfull parameters are used to derive other variables. This unavoidably inflates the margin of error for the methods detailed above. Additionally, this study assumes the Ningar River is representative of páramo rivers. Due to the high spatial variability of the northern Andes (Guzmán, Batelaan, Huysmans, & Wyseure, 2015; Luteyn, 1999), and the limited number of survey sites, it is unlikely that the Ningar River represents the full range of hydro-geomorphic variability in all páramo ecosystems.

Conclusions

It is interesting to see tacit agreement between the geomorphic methods established for equilibrated river systems and the models we derived for the Ningar River, which is located in an active tectonic setting and not likely to be equilibrated. The evidence for this agreement can be seen in several relatively strong r^2 values for our models and the agreement between our coefficients and the derivation proposed by Leopold and Maddock. It is also interesting to see that the Ningar River fits somewhat smoothly into Rosgen's classification system for an un-equilibrated river system. Perhaps the most compelling relationship developed is the τ_c model, not for the strength of its fit but the weakness. This relationship had the weakest r^2 of any of the power relationships, even though the relationships for the two other hydraulic variables were some of the strongest. Reaches of the Ningar River are expected to experience variable rates of erosion and deposition.

The páramo ecosystem provides numerous important ecosystem services including carbon sequestration, in the form of soil carbon, and water supply. Although this study has generated valuable information, the importance of the water resources of the páramo for the region and downstream linkages dictates that future research be undertaken to further develop regional hydro-

geomorphic curves for the páramo ecosystem, in order to refine these relationships. Considering the extensive dam building campaign underway in the northern Andes, and increasing population pressures, it is important to know that the hydro-geomorphic theories and models that have been developed and applied to other mountain-region river systems, also apply in the Ningar River, and likely other páramo systems.

In this study, we have provided a morphological description of a river system that drains an ecosystem for which fluvial geomorphic information has not yet been produced. We have shown that the hydrogeomorphology of the páramo grassland behaves similarly to other grassland and plains areas where the slope is low, and more typical of wet mountain systems with increased slope. By placing the Ningar River within the context of known river system morphologies, future research aimed at understanding tangential hydrologic and geomorphic processes such as environmental flows, bank erosion, and even fluvial carbon flux, will greatly benefit.

Bibliography

Baruch, Z. (1984). Ordination and classification of vegetation along an altitudinal gradient in the Venezuelan Páramos. *Vegetation*, *55*(2), 115–126. Retrieved from http://www.jstor.org/stable/20146032

Beniston, M. (2003). Climatic change in mountain regions: A review of possible impacts. *Climatic Change*, *59*(1–2), 5–31. Retrieved from http://doi.org/10.1023/A:1024458411589

Bieger, K., Rathjens, H., Allen, P. M., & Arnold, J. G. (2015). Development and evaluation of bankfull hydraulic geometry relationships for the physiographic regions of the United States. *Journal of the American Water Resources Association*, *51*(3), 1–17. Retrieved from http://doi.org/10.1111/jawr.12282

Bradley, R. S., Vuille, M., Diaz, H. S., & Vergara, W. (2006). Threats to water supplies in the tropical Andes. *Science*, *312*, 1755–56.

Bristow, C. R. (1973). *Guide to the geology of the Cuenca Basin, Southern Ecuador*. Quito: Ecuadorian Geological and Geophysical Society.

Buytaert, W., Célleri, R., Bièvre, D. B., Cisneros, F., Wyseure, G., Deckers, J., & Hofstede, R. (2006). Human impact on the hydrology of the Andean páramos. *Earth-Science Reviews*, *79*, 53–72. Retrieved from http://doi.org/10.1016/j.earscirev.2006.06.002

Buytaert, W., Deckers, J., & Wyseure, G. (2006). Description and classification of nonallophanic Andosols in south Ecuadorian alpine grasslands (páramo). *Geomorphology, 73 (3-4),*207-221. Retrieved from http://doi.org/10.1016/j.geomorph.2005.06.012

Buytaert, W., Deckers, J., & Wyseure, G. (2007). Regional variability of volcanic ash soils in south Ecuador: The relation with parent material, climate and land use. *Catena,70,* 143-154. Retrieved from http://doi.org/10.1016/j.catena.2006.08.003

Buytaert, W., Iñiguez, V., & Bièvre, B. De. (2007). The effects of afforestation and cultivation on

water yield in the Andean páramo. *Forest Ecology and Management, 251,* 22-30. Retrieved from http://doi.org/10.1016/j.foreco.2007.06.035

Caine, N., & Mool, P. K. (1981). Channel geometry and flow estimates for two small mountain streams in the Middle Hills, Nepal. *Mountain Research and Development*, *1*(3/4), 231–243.

Castro, J. M., & Jackson, P. L. (2001). Bankfull discharge recurrence intervals and regional hydraulic geometry relationships: Patterns in the Pacific Northwest, USA. *Journal of the American Water Resources Association*, *37*(5), 1249–1262.

Célleri, R., & Feyen, J. (2009). The hydrology of tropical Andean ecosystems : Importance , knowledge, status, and perspectives. *Mountain Research and Development*, *29*(4), 350–355. Retrieved from http://doi.org/10.1659/mrd.00007

Chang, H. H. (1988). *Fluvial processes in river engineering*. Malabar, Florida: Krieger Publishing Company.

Crespo, P., Celleri, R., Buytaert, W., Feyen, J., Iñiguez, V., Borja, P., & De Bievre, B. (2009). Land use change impacts on the hydrology of wet Andean páramo ecosystems. In A. Herrmann & S. Schumann (Eds.) *Status and Perspectives of Hydrology in Small Basins*. Retrieved from http://doi.org/10.13140/2.1.5137.6320

Dai, A., & Trenberth, K. E. (2002). Estimates of freshwater discharge from continents: Latitudinal and seasonal variations. *Journal of Hydrometeorology*, *3*(6), 660–687. http://doi.org/10.1175/1525-7541(2002)003<0660:EOFDFC>2.0.CO;2

Devol, A. H., & Hedges, J. I. (2001). Organic matter and nutrients in the mainstem Amazon River. In M. E. McClain, R. L. Victoria, & J. E. Richey (Eds.),*The biogechemistry of the Amazon basin.* (pp. 275–306). Oxford: Oxford University Press.

Dingman, S. L. (2007). Analytical derivation of at-a-station hydraulic–geometry relations. *Journal of Hydrology*, *334*(1–2), 17–27. Retrieved from http://doi.org/10.1016/j.jhydrol.2006.09.021

Dinnerstein, E., Olson, D. M., Graham, D. J., Webster, A. L., Primm, S. A., Bookbinder, M. P., & Ledec, G. (1995). *A conservation assesment of the terrestrial ecoregions of Latin America and the Caribbean*. Washington D.C.:The World Bank.

Dunne, T., & Leopold, L. B. (1978). *Water in environmental planning*. New York, New York: Freeman and Company.

EMAPAL. (2012). *Memoria técnica proyecto PUMA*. Azogues: Instituto Nacional de Preinversión.

FAO. (2003). *Review of world water resources by country*. *FAO Technical Paper* (Vol. 23). Rome. Retrieved from ftp://ftp.fao.org/agl/aglw/docs/wr23e.pdf

Farley, K. A., Kelly, E. F., & Hofstede, R. G. M. (2004). Soil organic carbon and water retention after conversion of grasslands to pine plantations in the Ecuadorian Andes. *Ecosystems,7, (7),* 729-739. Retrieved from http://doi.org/10.1007/s10021-004-0047-5

Finer, M., & Jenkins, C. N. (2012). Proliferation of hydroelectric dams in the Andean Amazon and implications for Andes-Amazon connectivity. *PLoS ONE*, *7*(4), 1–9. Retrieved from http://doi.org/10.1371/journal.pone.0035126

Gade, D. W. (1999). *Nature and culture in the Andes* (1st ed.). Madison, WI: University of Wisconsin Press.

Gibbs, R. J. (1967). The geochemistry of the Amazon River System: Part I. The factors that control the salinity and the composition and concentration of the suspended solids. *Geological Society of America Bulletin*, *78*(10), 1203. Retrieved from http://doi.org/10.1130/0016-7606(1967)78[1203:TGOTAR]2.0.CO;2

Gilvear D.J. (1999). Fluvial geomorphology and river engineering: Future roles utilizing a fluvial hydrosystem framework. *Geomorphology*, *31*, 229–245.

Guzmán, P., Batelaan, O., Huysmans, M., & Wyseure, G. (2015). Comparative analysis of baseflow characteristics of two Andean catchments, Ecuador. *Hydrological Processes, 29,* 3051-3064. Retrieved from http://doi.org/10.1002/hyp.10422

Harden, C. P. (2006). Human impacts on headwater fluvial systems in the northern and central Andes. *Geomorphology, 79,* 249-263. Retrieved from http://doi.org/10.1016/j.geomorph.2006.06.021

Harden, C. P., Hartsig, J., Farley, K. A., Lee, J., & Bremer, L. L. (2013). Effects of land-use change on water in Andean Páramo grassland soils. *Annals of the Association of American Geographers*, *103*(2), 375–384.

Hofstede, R. G. M., Groenendijk, J. P., Coppus, R., Fehse, J. C., & Sevink, J. (2002). Impact of pine plantations on soils and vegetation in the Ecuadorian High Andes. *Mountain Research and Development*, *22*(2), 159–167. Retrieved from http://dx.doi.org/10.1659/0276-

Hofstede, R., Segarra, P., & Vásconez, P. M. (2003). *Los Páramos del Mundo*. Proyecto Atlas Mundial de los Páramos. Global Peatland Initiative/NC-IUCN/EcoCiencia. Quito.

Huang, H. Q., & Nanson, G. C. (1997). Vegetation and channel variation; A case study of four small streams in southeastern Australia. *Geomorphology*, *18*(3–4), 237–249. Retrieved from http://doi.org/10.1016/S0169-555X(96)00028-1

Hungerbuhler, D., Steinmann, M., Winkler, W., Seward, D., Eguez, A., Peterson, D. E., … Winkler, W. (2002). Neogene stratigraphy and Andean geodynamics of southern Ecuador. *Earth-Science Reviews*, *57*, 75–124. Retrieved from www.elsevier.comrlocaterearscirev

Lave, R. (2009). The controversy over natural channel design: Substantive explanations and potential avenues for resolution. *Journal of the American Water Resources Association, 45, (6)* 1519-1532,. Retrieved from http://doi.org/10.1111/j.1752-1688.2009.00385.x

Leopold, L. B., & Maddock, T. (1953). *The hydraulic geometry of stream channels and some physiographic implications*. Washington D.C: United States Geological Survey.

Leopold, L. B., Wolman, M. G., & Miller, J. P. (1964). *Fluvial processes in geomorphology*. New York, New York: Dover Publications Inc.

Luteyn, J. L. (1999). *Páramos: A checklist of plant diversity, geographical dstribution, and*

botanical literature. Bronx, New York, New York: Botanical Garden Press.

Madriñán, S., Cortés, A. J., & Richardson, J. E. (2013). Páramo is the world's fastest evolving and coolest biodiversity hotspot. *Frontiers in Genetics*, *4*, 1–7. Retrieved from http://doi.org/10.3389/fgene.2013.00192

Mejía S., G. J., & Posada G., L. (2002). Geometría hidráulica para corrientes estables de la zona Andina Colombiana. In *XV Seminario Nacional de Hidráulica e Hidrología* (pp. 1-10). Medellin: Universidad Nacional de Colombia.

Mena Vásconez, P., & Hofstede, R. (2006). Los páramos ecuatorianos. In M. Moraes, B. Øllgaard, L. P. Kvist, F. Borchsenius, & H. Balslev (Eds.), *Botánica económica de los Andes Centrales* (pp. 91–109). La Paz, Bolivia: Universidad Mayor de San Andrés.

Messerli, B., Viviroli, D., & Weingartner, R. (2004). *Mountains of the World: Vulnerable Water Towers for the 21st Century*. *Ambio Special Report Number 13* (13). Retrieved from http://www.jstor.org/stable/25094585

Miller, J. R., & Ritter, J. B. (1996). An examination of the Rosgen classification of natural rivers. *Catena, 27,*295-299. Retrieved from http://doi.org/10.1016/0341-8162(96)00017-3

Milliman, J. D., & Meade, R. H. (1983). World-wide delivery of river sediment to the oceans. *The Journal of Geology*, *91*(1), 1–21. Retrieved from http://doi.org/10.1086/628741

Milliman, J. D., & Syvitski, J. P. M. (1992). Geomorphic/tectonic control of sediment discharge to the ocean: The importance of small mountainous rivers. *Journal of Geology*, *100, (1),* 525-544.

Modrick, T. M., & Georgakakos, K. P. (2014). Regional bankfull geometry relationships for southern California mountain streams and hydrologic applications. *Geomorphology*, *221*, 242–260. Retrieved from http://doi.org/10.1016/j.geomorph.2014.06.004

Montgomery, D. R., & Buffington, J. M. (1997). Channel-reach morphology in mountain drainage basins. *Bulletin of the Geological Society of America*, *109*(5), 596–611. Retrieved from

http://doi.org/10.1130/0016-7606(1997)109<0596:CRMIMD>2.3.CO

Nanzyo, M., Dahlgren, R., & Shoji, S. (1993). Chemical characteristics of volcanic ash soils. *Developments in Soil Science*, *21*, 145–187. Retrieved from http://doi.org/10.1016/S0166-2481(08)70267-8

Neirop, K. G. J., Tonneijck, F. H., Jansen, B., & Verstraten, J. M. (2007). Organic matter in volcanic ash soils under forest and páramo along an Ecuadorian altitudinal transect. *Soil Science Society of America Journal*, *71*, 1119–27.

Poulenard, J., Podwojewski, P., & Herbillon, A. J. (2003). Characteristics of non-allophanic Andisols with hydric properties from the Ecuadorian páramos. In *Geoderma, 117,* 267-281. Retrieved from http://doi.org/10.1016/S0016-7061(03)00128-9

Poulenard, J., Podwojewski, P., Janeau, J. L., & Collinet, J. (2001). Runoff and soil erosion under rainfall simulation of Andisols from the Ecuadorian Páramo: Effect of tillage and burning. *Catena, 45,* 185-207. Retrieved from http://doi.org/10.1016/S0341-8162(01)00148-5

Richards, K. (1982). *Rivers: Form and process in alluvial channels*. New York, New York: Blackburn Press.

Rosgen, D. L. (1994). A classification of natural rivers. *Catena*, *22,*169-199.

Rosgen, D. L. (1996). *Applied river morphology.* Pagosa Springs, Colorado: Wildland Hydrology.

Stewardson, M. (2005). Hydraulic geometry of stream reaches. *Journal of Hydrology, 306,* 97-111. Retrieved from http://doi.org/10.1016/j.jhydrol.2004.09.004

Team, R. Core. (2016). *R: A language and environment for statistical computing*. Vienna Austria: R Foundation for Statistical Computing. Retrieved from https://www.r-project.org/

Townsend-Small, A., McClain, M. E., Hall, B., Noguera, J. L., Llerena, C. A., & Brandes, J. A. (2008). Suspended sediments and organic matter in mountain headwaters of the Amazon River: Results from a 1-year time series study in the central Peruvian Andes. *Geochimica et Cosmochimica Acta*, *72*(3), 732–740. Retrieved from

http://doi.org/10.1016/j.gca.2007.11.020

Viviroli, D., & Weingartner, R. (2004). The hydrological significance of mountains: From regional to global scale. *Hydrology and Earth System Sciences*, *8*(6), 1017–1030. Retrieved from http://doi.org/10.5194/hess-8-1017-2004

Western, A. W., Finlayson, B. L., McMahon, T. A., & O'Neill, I. C. (1997). A method for characterising longitudinal irregularity in river channels. *Geomorphology*, *21*(1), 39–51. Retrieved from http://doi.org/10.1016/S0169-555X(97)00023-8

White, S. (2013). Grass paramo as hunter-gatherer landscape. *Holocene*, *23*(6), 898–915. Retrieved from http://doi.org/10.1177/0959683612471987

Wohl, E. E. (2000). *Mountain rivers* (14th ed.). Washington D.C.: American Geophysical Union.

Wohl, E. E., & Wilcox, A. (2005). Channel geometry of mountain streams in New Zealand. *Journal of Hydrology, 300,* 252-266. Retrieved from http://doi.org/10.1016/j.jhydrol.2004.06.006

Wohl, E., & Merritt, D. M. (2008). Reach-scale channel geometry of mountain streams. *Geomorphology, 93,* 168-185. Retrieved from http://doi.org/10.1016/j.geomorph.2007.02.014

Wolman, M. G. (1954). A method of sampling coarse river-bed material. *Transactions of the American Geophysical Union*, *35*(6), 951–956.

Yanchapaxi, G., Miranda, J. R., Colmet-Daage, F., & Zebrowski, C. (1983). *Cañar: Mapa de Suelos.* Quito: Ministerio de Agricultura y Ganadería.

Appendix 1: Cross Section Data

NR-1

XS-1

Tape (m)	Rod (m)
0	0.3
1	0.4
1.6	0.68
2.3	1
3	1.35
3.6	1.68
4	1.93
4.4	2.28
	2.44
5.15	2.57
5.75	2.53
6.7	2.33
7.2	2.28
7.9	2.28
8.45	2.26
8.3	1.12
8.6	1.74
9	1.69
9.7	1.33
11.5	0

XS-2

Tape (m)	Rod (m)
0	0.48
1.2	0.95
2.9	1.69
4.7	1.83
5.2	2.45
6.1	2.62
6.15	2.76
6.85	2.7
7.3	2.89
8.3	3
9.55	2.88
10.5	2.82
11.2	2.85

13	2.52
13.6	2.32
14.5	2.12
15.7	1

XS-3

Tape (m)	Rod (m)
0	0.58
2.05	1.45
4.5	1.69
4.9	1.72
5.5	1.94
5.85	2.14
6.6	2.33
7.3	2.19
7.55	2.29
7.75	2.75
8.35	2.84
8.85	2.92
9.5	2.89
9.9	2.95
10.2	1.63
10.9	1.66
11.65	1.66
12.7	1.42
14	0.75

NR-2

XS-1

Tape (m)	Rod (m)
0	0.77
0.7	0.78
0.9	1.79
1.3	1.84
1.9	1.92
2.5	1.87
3	1.86
3.7	1.85
	1.75
5.75	0.71
6.2	0.65

XS-2

Tape (m)	Rod (m)
7.2	0.32
6.3	0.53
5.9	0.57
5.6	1.71
5.2	1.68
4.5	1.54
3.95	1.68
3.55	1.65
3.2	1.7
2.7	1.63
2.4	1.6
	1.49
2	0.85
1.2	0.79
0	0.64

XS-3

Tape (m)	Rod (m)
0	0.4
1	0.47
2	0.64
3	0.92
3.3	1.6
3.6	1.75
4.1	1.84
4.6	1.96
5.1	1.97
5.6	1.94
	1.75
5.9	1.04
6.6	0.054

NR-3

XS-1

Tape (m)	Rod (m)
12.2	1.19
11.9	1.49
11.4	1.69

10.8	2.01
10.7	2.26
10.7	2.32
9.9	2.36
8.8	2.47
8.3	2.48
7.6	2.30
7.6	2.27
7.4	1.30
4.9	0.88
4.1	0.94
2.2	1.07
0	0.88

XS-2

Tape (m)	Rod (m)
13.5	0.60
11.9	1.15
9.4	1.30
8.6	1.69
8.5	2.47
8.5	2.63
7.5	2.56
6.8	2.52
5.6	2.49
5.6	2.46
5.3	1.87
4.8	1.58
3.6	1.37
0.9	1.34

XS-3

Tape (m)	Rod (m)
8	0.70
7.1	1.37
5.8	1.80
5.6	2.62
5.6	2.85
4.6	2.77
3.5	2.83
2.3	2.64
2.3	2.59

1.7	2.10
0	1.61

NR-4

XS-1

Tape (m)	Rod (m)
0	3.01
1.8	3.09
3.3	3.53
3.6	4.29
3.7	4.64
3.7	4.75
5	4.75
5.6	4.72
6.2	4.79
7.6	4.69
7.6	4.59
8.4	3.44
11.5	3.11
13.6	3.18
16	4.74

XS-2

Tape (m)	Rod (m)
0	1.65
2.3	1.49
4	1.56
4.4	2.84
4.9	3.44
6.2	4.13
7.3	4.59
7.4	5.01
7.4	5.03
7.6	5.13
8	5.03
8	5.00
8.7	4.85
9.5	5.00
9.5	5.03
10.8	5.22
11.5	5.29

12.9	5.12
13.7	5.19
13.7	5.02
14.1	3.69
15	3.42
18.4	3.31

XS-3

Tape (m)	Rod(m)
0	1.99
1.4	1.93
7.3	2.73
7.4	3.09
9.6	3.87
10	4.00
10.1	5.11
10.8	5.14
11.5	5.17
11.6	5.25
12.5	5.40
13.3	5.36
13.3	5.36
14.6	3.96
18.3	3.39

NR-5

XS-1

Tape (m)	Rod (m)
0	0.62
0.55	0.78
1	0.89
1.55	1.52
2.1	2.04
2.2	2.74
2.8	2.68
3.8	2.68
4.5	2.62
6	2.48
6.1	1.96
6.6	1.44
6.7	0.8

XS-2

Tape (m)	Rod (m)
0	0.67
0.5	0.67
1	0.63
1.5	0.83
2.55	2.14
2.75	2.24
4	2.43
4.95	2.37
6.05	2.3
6.25	2.24
6.7	1.1

XS-3

Tape (m)	Rod (m)
0	0.54
0.3	0.84
0.6	1.06
1.2	1.56
1.2	2.28
1.65	2.47
2.05	2.54
3	2.5
3.55	2.49
4.9	2.3
5.55	1.86
5.8	0.98

NR-6

XS-1

Tape (m)	Rod (m)
0	0.27
0.5	0.97
3.2	1.29
4.8	1.37
5.8	1.97
6.5	2.15
7	2.76
7.3	2.85

7.8	3.03
7.8	3.51
7.9	3.90
8.4	3.53
8.8	3.54
9.5	3.90
10	3.91
10.7	3.78
11.4	3.69
11.4	3.55
11.8	3.52
11.9	2.34

XS-2

Tape (m)	Rod (m)
0	1.16
2.3	2.40
2.9	2.65
3.5	3.94
3.51	3.99
4.4	4.04
5	4.16
5.7	4.43
6.4	4.48
7.2	4.50
7.7	4.05
7.7	4.24
8.6	2.43
9.1	1.82
11.6	1.09
12.5	1.00
13.1	0.69

XS-3

Tape (m)	Rod (m)
0	0.97
0.3	1.23
1	1.58
1.2	2.03
2.3	2.18
2.8	2.28
3.1	2.26

3.8	2.61
5	2.55
6.1	2.58
6.1	2.02
6.4	1.18
7.3	0.94
7.8	0.45

NR-7

XS-1

Tape (m)	Rod (m)
0	0.24
1.9	1.16
4.2	1.10
5.5	1.37
6.6	1.63
7.1	2.04
7.2	2.36
7.2	2.56
8.2	2.49
9	2.82
9.9	2.42
10.9	2.56
10.9	2.33
11	2.10
11.4	1.40
11.8	0.99

XS-2

Tape (m)	Rod (m)
0	0.49
0.7	1.56
4.9	1.74
6.3	1.67
7.8	1.87
8.1	2.26
8.5	2.20
8.6	2.93
8.6	3.54
9	3.78
9.9	3.72

10.3	3.81
10.6	3.76
11.1	3.91
11.5	3.99
11.7	3.94
12.4	3.87
12.9	3.52
12.9	3.35
13.2	2.37
14.4	2.27

XS-3

Tape (m)	Rod (m)
0	2.17
1.3	2.86
3	2.78
6.6	3.02
6.7	3.15
7.1	3.29
7.2	4.18
7.2	4.23
8.3	4.57
8.9	4.56
9.4	4.63
10.1	4.61
10.2	4.41
11.2	4.36
11.5	4.31
11.5	4.21
11.8	3.41
12.6	3.22
13.1	2.50
13.3	2.32

NR-8

XS-1

Tape (m)	Rod (m)
0	1.19
0.15	2.36
0.85	2.5
1.4	2.6

2.2	2.78
2.7	2.64
3.3	1.22
3.65	2.49
4.35	2.24
4.7	0.92
5	0.89
9	0.89

XS-2

Tape (m)	Rod (m)
0	0.9
0.4	2.26
0.9	2.2
1.3	2.44
1.75	2.24
2.2	2.31
2.7	2.32
3.1	2.02
3.9	2.1
4	1.23
4.5	0.86
4.8	0.88
20.4	0.88

XS-3

Tape (m)	Rod (m)
0	0.54
0.3	1.59
0.75	1.66
1.5	1.87
2.5	1.88
3.1	1.59
3.55	1.74
4	1.78
4.4	1.72
5.2	1.6
5.7	1.54
6.7	1.28
7	0.64
7.25	0.74
9.4	0.59

11.5	1
14.8	0.54
17.4	0.25

T-1

XS-1

Tape (m)	Rod (m)
0	0.44
0.25	0.48
0.5	0.69
0.95	1.3
1.15	1.22
1.3	1.85
1.6	1.84
2.1	1.86
2.55	1.83
3.05	1.83
	1.69
3.35	0.28

XS-2

Tape (m)	Rod (m)
0	0.3
0.25	0.36
0.45	0.36
0.6	1.65
1	1.64
1.7	1.77
2.15	1.54
2.55	1.34
3.1	3.09

XS-3

Tape (m)	Rod (m)
0	1.26
0.3	1.27
0.6	1.38
0.75	2.09
0.9	2.13
1.4	2.27

2.15	2.42
2.4	2.56
2.7	2.51
2.9	2.45
3	1.96
3.55	1.06

T-2

XS-1

Tape (m)	Rod (m)
0	0.14
0.5	1.12
1.1	1.23
2.2	1.52
4.9	1.75
5	2.54
5.5	2.64
5.9	2.77
6.4	2.75
6.6	2.75
6.8	2.38
7.1	1.85
7.7	1.55
12.4	1.64
14.3	0.89
16.8	1.51
26	1.56
28.4	0.90
29.4	0.62

XS-2

Tape (m)	Rod (m)
0	2.43
1.3	2.46
10.6	2.26
11.4	2.67
12	3.44
12.1	3.60
12.9	3.68
13.9	3.54
14.1	2.83

14.6	2.58
17.4	2.82
18.6	2.76
20.8	2.57
21.8	2.49
22.2	1.58

XS-3

Tape (m)	Rod (m)
0	0.31
1.7	0.47
4.4	1.70
7.1	2.31
7.4	3.53
7.41	3.81
7.9	3.85
8.4	3.86
9.2	3.76
9.7	3.64
10.2	3.66
10.2	3.53
10.3	3.06
11	2.75
14.7	2.71
17.3	2.77

Appendix 2: Longitudinal Profile Data

NR-1

Tape (m)	Rod (m)
0	2.2
2	2.38
3.4	2.05
5.2	2.17
6.1	2.06
7	1.92
7	1.78
8.4	1.91
7.8	1.9
10.6	1.96
13.65	2.15
13.9	2.18
13.9	1.94
15.95	2.22
17.75	2.04
20	2.14
22	1.96
22	1.79
23.5	1.98
24.35	2.06
24.9	2.02
27	2.15
28.75	2.22
28.75	1.42
29.3	1.4
29.7	1.52
30.4	1.6
31.3	1.64
32.6	1.6
33.75	1.54
34.8	1.53
35.3	1.48
36.5	1.58
37.7	1.52
37.7	1.38
38.8	1.54
39	1.58
40.3	1.78

41.15	1.67
42.5	1.7

NR-2

Tape (m)	Rod (m)
0	2.1
2.75	2.1
5.3	1.96
6.6	2
6.6	1.85
7.6	2
8.2	2.07
10.3	2.22
11.5	2.25
14	2.14
14	1.96
15.4	2.2
15.5	2.2
15.5	1.8
17.5	2.24
19.7	2.3
20.5	2.39
21.3	2.38
22.3	2.36
23.7	2.22
25.6	2.24
26.75	2.24
29.1	2.3
31.7	2.33
31.7	3.1
36.2	3.55
38.6	3.52
40.3	3.6
41.8	3.6
43.6	3.65
44.4	3.55
45.6	3.65
47.2	3.42
47.2	3.28
47.5	3.44
47.9	3.45
49.4	3.55
51.15	3.51

53	3.59
53	1.67
53.6	1.66
54.2	1.68
55.4	1.74
57.4	1.77
59.3	1.78
59.5	1.79
60.7	2.04
61.6	2.05
63.2	2.97
65	2.05
66.3	2.24
67.7	2.3

NR-3

Tape (m)	Rod (m)
0	2.50
1.9	2.51
3.6	2.49
4	2.47
6.5	2.46
7	2.65
13	3.06
14.4	2.93
16.2	2.85
17.9	2.92
19.8	3.00
25.4	2.65
28.9	2.23
29	3.02
31	2.74
32.4	2.86
35.4	3.25
37.6	3.19
41.1	3.29
49.4	3.26
49.9	3.44
55.4	2.83
56.7	2.76
59	2.88
60.2	3.36
61.8	3.35

63.9	3.07
66	3.20
71.4	3.17
74.7	3.14
78.8	3.23
80.1	3.36
82.7	3.41
84.3	3.47
87.7	3.41
89.2	3.55
91.5	3.61
92.8	3.52
96.9	3.56
100	3.69

NR-4

Tape (m)	Rod (m)
0.00	5.09
4.30	4.85
5.40	4.79
6.00	4.80
9.30	4.86
9.80	4.96
11.70	5.12
12.60	5.23
15.50	5.25
18.40	5.25
21.50	5.25
25.60	5.17
27.70	5.16
29.00	5.27
30.60	5.67
32.40	6.00
35.60	5.42
36.20	5.24
37.40	5.24
38.80	5.48
41.30	5.50
43.40	5.70
44.50	5.85
45.90	5.86
48.60	5.50

50.40	5.41
52.60	5.40
53.30	5.36
56.00	5.44
59.40	5.55
60.50	5.65
62.30	5.85
65.60	5.76
69.10	5.78
72.40	5.75
77.20	5.80
79.60	5.76
82.80	5.96
86.30	6.38
88.20	6.28
90.60	6.03
92.30	5.82
93.40	6.09
95.60	6.43
96.40	6.64
98.50	6.68
100.00	6.60

NR-5

Tape (m)	Rod (m)
0	3.2
0.5	3.06
3.5	2.8
3.5	2.45
7.2	2.68
8.7	2.64
12.5	2.66
14.3	2.8
15.5	2.75
17.8	2.7
19.8	2.75
19.8	3.38
23.3	3.5
25	3.35
27.6	3.4
27.6	3.18
31	3.41

33.6	3.38
36.5	3.62
36.5	3.78
39.5	3.95
42.8	3.77
46.7	3.86
47	4.1
47	4.1
49.8	4.14
52	3.98
	4
55.2	3.86
60	3.96
62.4	3.86
	3.5
64.1	3.77
66.2	3.67
	3.69
69	3.39
71.5	3.66
72.8	3.7
74	3.64
76.2	3.64
77.3	3.55
79.4	3.67
81.3	3.7
85	3.66

NR-6

Tape (m)	Rod (m)
32	4.19
24.9	3.33
21.7	3.32
21.71	4.08
20	4.43
16.4	4.01
13.4	3.87
11.2	3.95
7.1	3.81
5.3	4.02
2	3.97
1	3.90

0	3.88
1.9	3.99
3.6	4.00
5.5	4.08
7.4	3.96
9	4.16
10.8	4.23
11.8	4.10
13.4	4.13
15	4.24
17.4	4.24
20.4	4.19
23	4.57
27.7	4.97
31.6	4.61
32.8	4.85
34.5	4.91
35.7	5.28
37.6	5.05
39.7	4.85
40.2	5.05
41.6	5.07
42.6	5.03
43.2	5.26
44.3	5.35
46.4	5.25
47	5.24
47.1	5.16
48.3	5.13
50.3	5.27
51.2	5.58
61.8	5.65
63	5.68

NR-7

Tape (m)	Rod (m)
0	2.44
3.3	1.97
3.4	2.56
4.3	2.66
5.4	2.69
8.1	2.82

9	2.89
11.9	2.71
14.5	2.98
16	2.54
16.7	2.68
18.1	2.79
19.5	3.11
21.6	2.88
22.2	2.97
23.5	3.16
25.6	3.10
26.9	3.22
28	3.54
29.1	3.33
30.9	2.91
32	3.29
33.4	3.51
35	3.12
38	4.33
41.4	4.22
49	4.39
49.2	4.11
52.3	3.99
54.4	3.99
55.1	4.02
55.6	3.99
56.6	4.01
58	4.24
58.9	4.33
59.5	4.32
61.7	4.34
63.8	4.40
65.6	4.52
66.2	4.56
70.3	4.82
73	4.63
74.6	4.58
75.8	4.64
76.6	4.80
77.7	4.97
79.2	5.04
82.1	4.95
84.5	4.95

86.7	5.02
87.7	5.01
89.5	5.43
92.1	5.10
93	5.32
94.4	5.43
95.2	5.76
96	5.69

NR-8

Tape (m)	Rod (m)
68	2.64
65.5	2.62
65	2.12
65	2.57
64.8	2.32
64.5	2.36
64.5	2.55
61.4	2.8
59.5	2.89
58.1	3
56.1	2.49
56.1	2.89
53	2.83
51.5	2.74
49.5	2.43
48.6	2.28
48.6	2.06
47.9	2.5
45	2.66
43.7	2.57
43.1	2.1
43.1	2.68
41.25	2.3
39.2	2.34
37.9	2.43
36.6	2.52
34.7	2.37
33.6	2.38
29.5	2.56
27.5	2.27
27.5	2.6

27.2	1.69
27.1	1.85
25.8	1.88
23.3	2
22.8	2.22
22.8	1.59
22.4	1.68
22.3	2
19.5	2.27
18.5	2.48
16.8	2.52
15	2.4

T-1

Tape (m)	Rod (m)
0	1.89
1	1.9
1.9	1.96
2.4	1.86
3.55	1.9
4.3	1.89
5.5	1.82
6.1	1.8
6.1	1.62
6.3	1.81
7.45	2.02
9	2.19
10.5	2.54
11.5	2.58
12.5	2.26
12.5	2.08
14.3	2.1
16	2.08
16.8	2.03
17.5	1.82
17.6	2
18.1	2.08
18.7	2.16
19.9	2.29
21	2.23
22.9	2.32
22.9	1.66

23.8	1.75
26.8	1.88
27.7	1.89
29	2.02
30.5	2.11
32	2.26
32	2.1
32.85	2.05
32.85	1.55
34.1	1.94
34.2	1.68
35	1.96
36.5	2.06
37.5	1.95
38.3	1.88
38.9	2.07
39.5	2.16
40	2.08
40.9	2.08
41.4	2.09
41.4	1.25
42.45	1.14
43.1	1.29
43.9	1.3
44.35	1.54
45.9	1.6
46.2	1.49
46.5	1.69
47.2	1.86
48.2	1.88
48.9	2.07
48.9	1.79
50.5	2.04

T-2

Tape (m)	Rod (m)
0	2.44
1.6	2.70
2.8	2.51
3.5	2.33
4	2.15
4.1	2.44

5	2.66
5.6	2.48
7.3	2.61
8.1	2.52
8.4	2.62
11	2.79
11.9	2.78
14.7	3.02
14.9	3.30
15.1	3.38
16.2	3.51
20.6	3.58
25.9	3.30
28	3.39
30.1	3.55
31.7	3.38
34	3.45
34.3	3.69
36.2	3.71
38.7	3.73
39.3	3.57
39.3	3.57
40	3.86
41.5	4.08
42.9	4.37
44	4.66
47.3	3.84
50.5	4.41
52.1	4.63
56.6	4.38
60	4.29
63.6	4.83
70.2	4.99
72.9	5.09
74.8	5.38
83.5	5.16
85.1	5.07
88.1	5.72
89	6.04
91.2	5.92
94.3	5.49
96.4	5.42
97.6	5.30

97.7	5.64
99.2	5.88
100	5.80

Vita

Christopher Palumbo Ely was born and raised in near-suburban Chicago. He grew up through the dot com bubble burst and barely survived the great recession. He developed an interest in the natural environment after spending a summer trying to catch a fish. He was not successful. Yet, he realized then he has always been fascinated by the natural world and sought to build career in the geosciences. He obtained a B.A. in Geology from Southern Illinois University Carbondale in 2015. While there he developed the skills to become a geoscientist and concentrated in geophysics and gem hunting. After graduating he was accepted into the graduate program in the Department of Geography and Planning at Appalachian State University and concentrated on fluvial geomorphology in the Andes and Appalachian Mountains. He has overcome much adversity in the pursuit of not being a perpetual screw up. He was told this thesis can be taken as proof of that, doubt remains however.